AFOSR - TR - 71-2182

VKI TN 75

AD 728244

von KARMAN INSTITUTE
FOR FLUID DYNAMICS

GRANT AF EOOAR 70 - 0082
Final Scientific Report
1 May 1970 - 30 April 1971
(Laminar Separation at Hypersonic Speeds)

CONE CAVITY FLOW AT M = 5.3 WITH INJECTION. EFFECT OF INCIDENCE

by

Jean J. GINOUX

and

Félix THIRY

VKI TN 75

DDC
RECEIVED
AUG 3 1971
A

Approved
Distribution

[redacted]

RHODE-SAINT-GENESE, BELGIUM

JUNE 1971

Reproduced by
NATIONAL TECHNICAL
INFORMATION SERVICE
Springfield, Va. 22151

61

Best
Available
Copy

UNCLASSIFIED
Security Classification

DOCUMENT CONTROL DATA – R & D

(Security classification of title, body of abstract and indexing annotation must be entered when the overall report is classified)

1. ORIGINATING ACTIVITY (Corporate author)
VON KARMAN INSTITUTE FOR FLUID DYNAMICS
1640 RHODE-ST-GENESE, BELGIUM

2a. REPORT SECURITY CLASSIFICATION
UNCLASSIFIED

2b. GROUP

3. REPORT TITLE
CONE CAVITY FLOW AT MACH 5.3 WITH INJECTION. EFFECT OF INCIDENCE

4. DESCRIPTIVE NOTES (Type of report and inclusive dates)
Scientific Final

5. AUTHOR(S) (First name, middle initial, last name)
JEAN J GINOUX FELIX THIRY

6. REPORT DATE
June 1971

7a. TOTAL NO. OF PAGES
53

7b. NO. OF REFS
8

8a. CONTRACT OR GRANT NO.
EOOAR -0082-70

b. PROJECT NO.
9781-02

c. 61102F

d. 681307

9a. ORIGINATOR'S REPORT NUMBER(S)
VKI TN 75

9b. OTHER REPORT NO(S) (Any other numbers that may be assigned this report) AFOSR - TR - 71-2182

10. DISTRIBUTION STATEMENT
Approved for public release; distribution unlimited.

11. SUPPLEMENTARY NOTES
TECH, OTHER

12. SPONSORING MILITARY ACTIVITY
AF Office of Scientific Research (NAM)
1400 Wilson Boulevard
Arlington, Virginia 22209

13. ABSTRACT

A previous experimental study of the favorable effect of mass injection into a hypersonic separated laminar flow on pressure and heat transfer distributions at reattachment has been extended to include the influence of a small incidence of the model. Measurements were made at M = 5.3 on a circular cone with an annular cavity, into which air was injected at rates up to approximately half the boundary layer mass flow at separation. Incidence was varied by halfdegree steps in the range zero to two degrees. The reattachment pressure and heat transfer peaks increased on the windward side with incidence and more mass injection was required to maintain them below a given level. The relative locations of these peaks were inverse at zero and two degrees incidence.

Details of illustrations in this document may be better studied on microfiche

DD FORM 1 NOV 65 1473

UNCLASSIFIED
Security Classification

GRANT [redacted] EOOAR 70-0082

FINAL SCIENTIFIC REPORT

LAMINAR SEPARATION AT HYPERSONIC SPEEDS

1 May 1970 - 30 April 1971

JEAN J.GINOUX

and

FELIX THIRY

Details of illustrations in
this document may be better
studied on microfiche

von KARMAN INSTITUTE FOR FLUID DYNAMICS
Rhode Saint Genèse, Belgium

Technical Note 75

~~This document has been approved for public release and sale; its distribution is unlimited.~~

This research has been sponsored in part by the Air Force Office of Scientific Research, through the European Office of Aerospace Research, OAR, U.S.Air Force, under Grant [redacted] EOOAR 70-0082

TABLE OF CONTENTS

SUMMARY ii
LIST OF FIGURES iii
LIST OF SYMBOLS v

1. INTRODUCTION 1

2. EXPERIMENTAL EQUIPMENT AND TEST TECHNIQUES . . 2
2.1 Wind tunnel 2
2.2 Models 2
2.3 Model adjustment 2
2.4 Test techniques and data reduction 3

3. RESULTS 5

4. CONCLUSIONS 8

REFERENCES 9

FIGURES

SUMMARY

A previous experimental study of the favorable effect of mass injection into a hypersonic separated laminar flow on pressure and heat transfer distributions at reattachment has been extended to include the influence of a small incidence of the model.

Measurements were made at M = 5.3 on a circular cone with an annular cavity, into which air was injected at rates up to approximately half the boundary layer mass flow at separation. Incidence was varied by half-degree steps in the range zero to two degrees.

The reattachment pressure and heat transfer peaks increased on the windward side with incidence and more mass injection was required to maintain them below a given level. The relative locations of these peaks were inverse at zero and two degrees incidence.

LIST OF FIGURES

1 Model configurations

a Pressure model

b Heat transfer model

2 Pressure distributions with and without air injection

2.1 $\alpha = 0$ $\theta = 0$

2.2 $\alpha = -30'$ $\theta = 0$

2.3 $\alpha = -1°$ $\theta = 0$

2.4 $\alpha = -1°30'$ $\theta = 0$

2.5 $\alpha = -2°$ $\theta = 0$

2.6 $\alpha = -30'$ $\theta = 45°$

2.7 $\alpha = -1°$ $\theta = 45°$

2.8 $\alpha = -1°30'$ $\theta = 45°$

2.9 $\alpha = -2°$ $\theta = 45°$

2.10 $\alpha = -30'$ $\theta = 90°$

2.11 $\alpha = -1°$ $\theta = 90°$

2.12 $\alpha = -1°30'$ $\theta = 90°$

2.13 $\alpha = -2°$ $\theta = 90°$

2.14 $\alpha = -30'$ $\theta = 180°$

2.15 $\alpha = -1°$ $\theta = 180°$

2.16 $\alpha = -1°30'$ $\theta = 180°$

2.17 $\alpha = -2°$ $\theta = 180°$

3 Heat transfer distributions with and without air injection

3.1 $\alpha = 0$ $\theta = 0$

3 2 $\alpha = -30'$ $\theta = 0$

3.3 $\alpha = -1°$ $\theta = 0$

3.4 $\alpha = -1°30'$ $\theta = 0$

3.5 $\alpha = -2°$ $\theta = 0$

3.6 $\alpha = -30'$ $\theta = 45°$

3.7 $\alpha = -1°$ $\theta = 45°$

3.8 $\alpha = -1°30'$ $\theta = 45°$

3.9 $\alpha = -2°$ $\theta = 45°$

3.10 $\alpha = -30'$ $\theta = 90°$
3.11 $\alpha = -1°$ $\theta = 90°$
3.12 $\alpha = -1°30'$ $\theta = 90°$
3.13 $\alpha = -2°$ $\theta = 90°$

3.14 $\alpha = -30'$ $\theta = 180°$
3.15 $\alpha = -1°$ $\theta = 180°$
3.16 $\alpha = -1°30'$ $\theta = 180°$
3.17 $\alpha = -2°$ $\theta = 180°$

4 Effect of air injection on maximum pressure ratio
4.1 $\theta = 0$
4.2 $\theta = 45°$
4.3 $\theta = 90°$
4.4 $\theta = 180°$

5 Effect of air injection on maximum heat transfer ratio
5.1 $\theta = 0$
5.2 $\theta = 45°$
5.3 $\theta = 90°$
5.4 $\theta = 180°$

LIST OF SYMBOLS

c_q	mass injection ratio defined in section 3
L	cavity width defined in figure 1
p	wall static pressure
p_c	cone pressure at zero incidence defined by formula (1)
$\bar{p}_c$	average cone pressure measured in a test series
q	wall heat flux
q_c	computed heat flux on a cone at zero incidence
Q_{BL}	boundary layer mass flow computed at separation
u	velocity of air in inviscid flow over a circular cone
x	surface distance defined in figure 1
x_m	location of pressure or heat transfer peaks
α	incidence
ρ	density of air in inviscid flow over a circular cone
θ	azimutal angle $\theta = 0$ windward side $\theta = 180$ leeward side

1. INTRODUCTION

For a number of years, it has been known that the presence of a cavity in the surface of a hypersonic body gives rise to a significant redistribution of surface pressure and heat transfer to the body (refs. 1, 2,3). Specifically, these quantities are reduced in the region of separated flow but experience a sharp rise within the vicinity of reattachment, followed by a decrease toward the undisturbed values in the downstream area. For practical applications, the primary undesirable feature of this phenomenon is the elevated pressure and heat transfer at reattachment. This fact justifies further research into methods of substantially reducing these peak values.

It has been previously theoretically predicted and experimentally verified that injection of a small amount of gas (a fraction of the mass flow in the boundary layer at separation is sufficient) into the separated region accomplishes this result (refs. 1, 4, 5, 6, 7).

The investigation of reference 6 was directed toward provision of detailed static pressure and heat transfer distributions over the entire surface of cone-cavity models with and without air injection into the cavity at a free stream Mach number of 5.3. Emphasis was given to the reattachment region by using a cavity with a rounded reattachment shoulder, as opposed to Nicoll's cavity (3 to 5) which had 90° sharp corners.

This work was extended in reference 7 to foreign gas injection. Light gases (helium and hydrogen) were found to be substantially more effective in reducing pressure and heat transfer peaks than air and much more so than heavy gases (freon and carbon tetrachloride vapor).

The purpose of the present study is to further extend this research to include the effect of a small incidence of the cone cavity model on the effect of air injection.

2. EXPERIMENTAL EQUIPMENT AND TEST TECHNIQUES

2.1 Wind tunnel

All experiments were conducted in the VKI hypersonic blowdown tunnel H-1 at a free stream Mach number of 5.3. The size of the test section is 12×12 cm^2, giving a uniform flow with $\pm \frac{1}{2}$ percent variation in Mach number. The stagnation temperature was about 220°C. The stagnation pressure was of about 15.4 kg/cm^2, corresponding to a free stream Reynolds number of 1.65×10^5 per centimeter.

2.2 Models

The basic model configuration is a 10° semi-apex angle cone incorporating an annular cavity of the short-deep type. Dimensions and details of the location of pressure taps and thermocouples are shown in figures 1a and 1b. Separate models were used for pressure and heat transfer measurements.

The injected air entered the cavity tangentially to the floor from an annular port (1 mm wide) located at the base of the reattachment shoulder. The detailed description of the injection plant is given in reference 7.

2.3 Model adjustment

At incidence, the flow over the model is no longer axisymmetric and it is desirable to obtain static pressure and heat transfer distributions along various generators of the model; say on the windward side ($\theta = 0$), at $\theta = 45°$ and 90° and on the leeward side ($\theta = 180°$).

On the present models, pressure taps and thermocouples are staggered on both sides of a single generator (see figures 1a and 1b). It was thus possible to obtain the desired information by rotating the model around its axis of symmetry by 45, 90 and 180 degrees; corrections being

made in each case (by data interpolation) to allow for the small stagger ($\theta = \pm 1°$ deg. maximum) of the pressure taps and thermocouples.

The main problem consisted of correctly defining the zero incidence of the model because of the great sensitivity of the pressure and heat transfer distributions in the reattachment region of the flow to a small angle of attack.

It was solved by the use of four pressure taps spaced by 90° and located in a cross plane at some distance downstream of the cavity ($p_0, p_{90}, p_{180}, p_{270}$). By rotating each of the models around its axis, the streamwise pressure and heat transfer distributions were successively measured at θ = 0, 90, 180 and 270 degrees, each time adjusting the incidence and yaw of the model so that $\Delta p = p_{180} - p_0 = 0$ and $\Delta p = p_{270} - p_{90} = 0$. From these, mean streamwise pressure and heat transfer distributions were selected that were used as standard references for zero incidence adjustment in all the subsequent tests. In other words, in each of these tests the model was adjusted in incidence so that the measured pressure or heat transfer distribution was identical (especially its peak value) to the standard one in the absence of gas injection into the cavity. Model incidence was then varied by 30' increments in the range 0 to 2 degrees.

2.4 Test techniques and data reduction

The test techniques are the same as described in reference 7. Pressure distributions were obtained with the aid of 12-tube rotary valves, a differential transducer and a digital printer. Heat transfer rates were measured using a thin skin technique and a 12-channel galvanometric recorder.

In the present report, all the pressure data is referenced to p_c which is the cone pressure (measured upstream of the cavity) at *zero incidence* ($\alpha = 0$), corrected in each test according to the formula

$$p_c(\alpha=0) = \frac{p_c(\alpha,\theta)}{\overline{p}_c(\alpha,\theta)}\,\overline{p}_c(\alpha=0) \qquad (1)$$

where $\overline{p}_c(\alpha=0)$ and $\overline{p}_c(\alpha,\theta)$ are the average values of $p_c(\alpha=0)$ and $p_c(\alpha,\theta)$ measured at different injection rates in a test series, either at $\alpha = 0$ or for given values of α and θ.

The heat transfer data (q) is normalized with the heat flux (q_c) computed on a pure cone at zero incidence, at the same distance from the nose, for the stagnation conditions measured during each test, assuming laminar flow and a recovery factor of 0.85.

3. RESULTS AND DISCUSSION

The pressure and heat flux ratios ($\frac{p}{p_c}$ and $\frac{q}{q_c}$) are shown in figures 2.1 to 2.17 and 3.1 to 3.17 versus x/L, for different injections rates c_q. For each incidence α of the model, the measurements were made at four different locations (θ = 0,45,90 and 180 degrees) around the model.

In these figures, x is the surface distance measured along a model generator with its origin at the junction of the reattachment shoulder and the aftercone, as shown in figure 1. L is the cavity width as defined in figures 1a and 1b; L = 12 mm was used in figures 2 and 3. c_q is the ratio of injected mass flow to the boundary layer mass flow Q_{BL} computed at separation on the model at zero incidence. Q_{BL} was of the order of 22 liters/minute, based on standard conditions (see ref. 7). One will note that different vertical scales are used in these figures.

The symbol TH indicates the asymptotic value of $\frac{p}{p_c}$ or $\frac{q}{q_c}$ that is theoretically reached on the aftercone at downstream infinity. Flow tables for cones at incidence were used to determine p_{TH} and $(\rho u)_{TH}$ as a function of α and θ (ref. 8), $(\rho u)_{TH}$ being used to compute q_{TH} from an expression of the Stanton number valid for circular cones at zero incidence .

The cavity pressure ratio is shown on the left portion of figures 2.1 to 2.17. It is observed that this ratio was not appreciably affected by model incidence. For zero injection (c_q = 0) for instance, it remained approximately equal to 0.9.

The effect of model incidence on the streamwise pressure and heat transfer distributions is rather obvious. Both pressure and heat transfer ratios are increased with incidence on the windward side (θ = 0) and at θ = 45°. They

are but little affected at $\theta = 90°$ and are decreased on the leeward side ($\theta = 180°$).

It is interesting to note the forward displacement (decreasing x) of the pressure and heat transfer peaks on the windward side of the model as the angle of attack is increased. Despite the uncertainty which obviously exists in defining the exact location of these peaks, it nevertheless appears that the location of the heat transfer peak moved faster than the pressure peak location. At zero incidence $(\frac{q}{q_c})_{max}$ is located slightly downstream of $(\frac{p}{p_c})_{max}$, while at $\alpha = -2°$, $(\frac{q}{q_c})_{max}$ has moved slightly upstream of $(\frac{p}{p_c})_{max}$. This is shown in the sketch where the location $(\frac{x}{L})_m$ of the peaks is plotted versus the model incidence α.

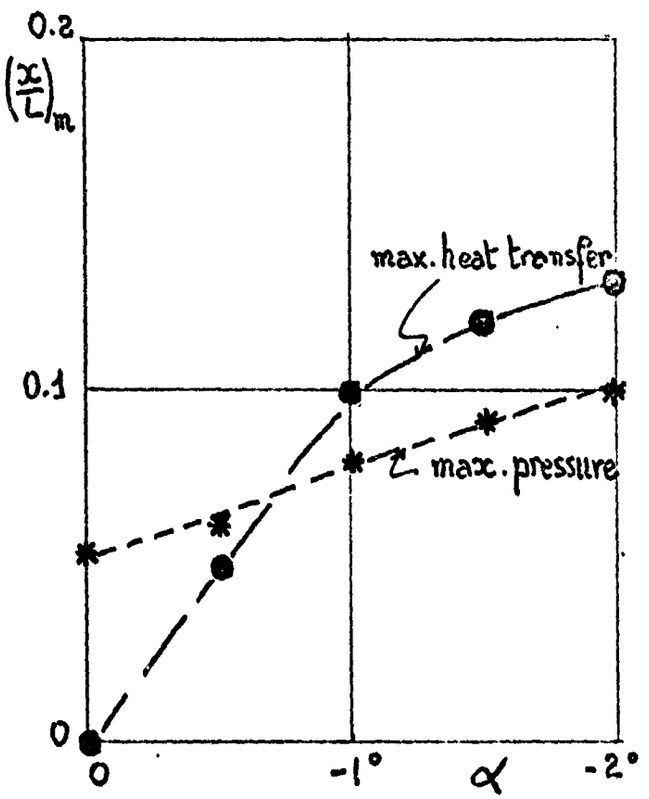

Transition to turbulent flow appeared sooner on the leeward side at incidence than for $\alpha = 0$. This is shown in figures 2.1 and 3.16 by the more rapid increase of $\frac{q}{q_c}$ with $\frac{x}{L}$ on the downstream portion of the model at $c_q = 0$.

The favorable effect of mass injection into the cavity was similar to the one observed in the previous study (ref. 7) made at zero incidence, namely that the pressure level and the heat transfer rate were decreased in the region of flow reattachment. This is particularly so for the pressure and heat transfer peaks as seen in figures 4.1 to 4.4 deducted from figures 2 and 3. Because of the higher values of these peaks on the windward side of the model, larger mass injection rates were needed at incidence than for $\alpha = 0$ to maintain the pressure and heat transfer ratios below specified levels. However, these rates remained of the order or less than the boundary layer mass flow at separation (i.e., very small for practical applications) in the range of incidence which was considered in the present study.

The locations of the pressure and heat transfer peaks were differently affected by mass injection. At zero incidence, the pressure peak remained fixed while the heat transfer peak moved downstream (x increasing) as c_q was increased. At incidence ($\alpha \neq 0$), $\left(\frac{p}{p_c}\right)_{max}$ moved downstream at $\theta = 0$ and $\theta = 45°$ and remained fixed at $\theta = 90$ by increasing c_q. At $\theta = 180$ the pressure peak was so faint that its location was difficult to define accurately. At incidence ($\alpha \neq 0$) $\left(\frac{q}{q_c}\right)_{max}$ moved downstream for all values of θ.

4. CONCLUSIONS

The favorable effect of mass injection observed previously on a cone-cavity model at zero incidence was reconfirmed at small angles of attack, in the range zero to two degrees. Pressure and heat transfer peaks at flow reattachment could indeed be maintained below specified levels by a small amount of air injection into the cavity, i.e., at rates of the order of the boundary layer mass flow at separation.

The effect of incidence without mass injection was to increase the pressure and heat transfer peaks on the windward side of the model and to decrease them on the leeward side. The relative locations of these peaks were inverse at zero and two degrees incidence.

REFERENCES

1. CHAPMAN, D.R.: A theoretical analysis of heat transfer in regions of separated flow.
NACA TN 3792, 1956.

2. LARSON, H.K.: Heat transfer in separated flow.
JAS vol. 26, pp 731-738, Nov. 1959.

3. NICOLL, K.M.: A study of laminar hypersonic cavity flows.
AIAA Jnl, vol. 2, No 3, pp 1535-1541, Sept. 1964.

4. NICOLL, K.M.: Mass injection in a hypersonic cavity flow.
ARL 65-90, May 1965.

5. NICOLL, K.M.: An experimental investigation of laminar hypersonic cavity flows. Part II - Heat transfer and recovery factor measurements.
ARL 63-73, January 1964.

6. GINOUX, J.J.: Laminar separation in hypersonic flows.
Grant AF EOAR 67-09, Final Scientific Report, November 1967.

7. GINOUX, J.J.: Cone cavity flow at M = 5.3 with injection of light, medium and heavy gases.
VKI TN 35, November 1968.

8. JONES, D.J.: Tables of inviscid supersonic flow about circular cones at incidence (γ = 1.4).
AGARDograph 137, November 1969.

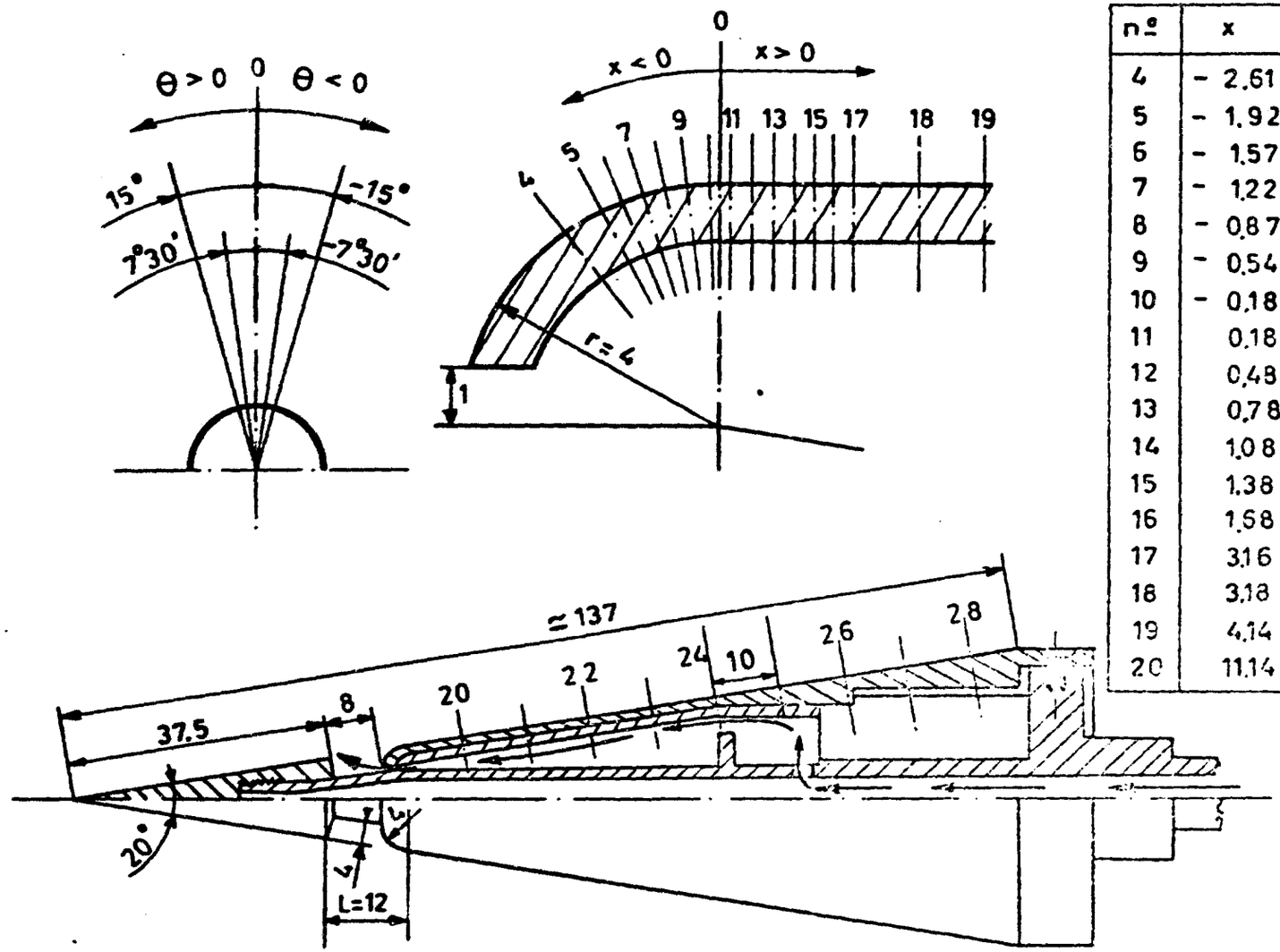

nº	x	θ
4	- 2.61	0
5	- 1.92	15
6	- 1.57	7°30
7	- 1.22	-7°30
8	- 0.87	-15
9	- 0.54	15
10	- 0.18	7°30
11	0.18	-7°30
12	0.48	-15
13	0.78	15
14	1.08	7°30
15	1.38	-7°30
16	1.68	-15
17	3.16	0
18	3.18	0
19	4.14	0
20	11.14	0

a. Pressure model

Fig. 1 MODEL CONFIGURATIONS.

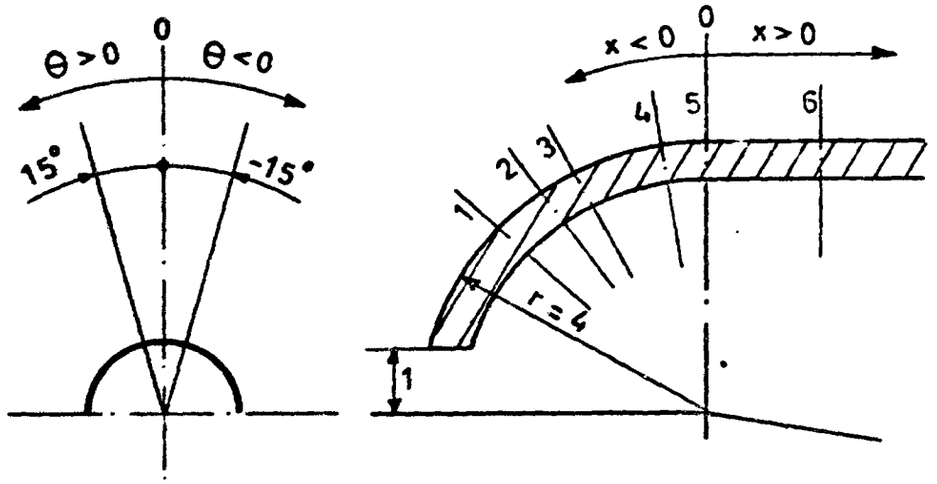

n°	x	θ
1	- 3,30	15
2	- 2,49	0
3	- 1,99	-15
4	- 0,69	15
5	0	0
6	1,59	0
7	3,20	0
8	7,99	0
11	13,20	0
13	23,10	0
14	36,36	0

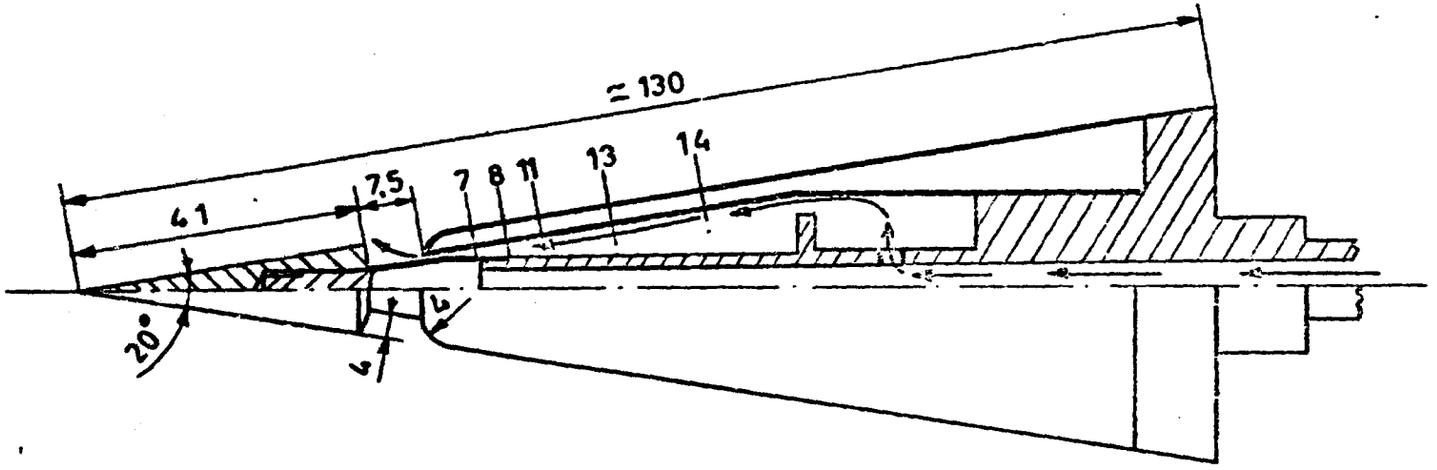

b. Heat transfer model.

Fig. 1 CONCLUDED.

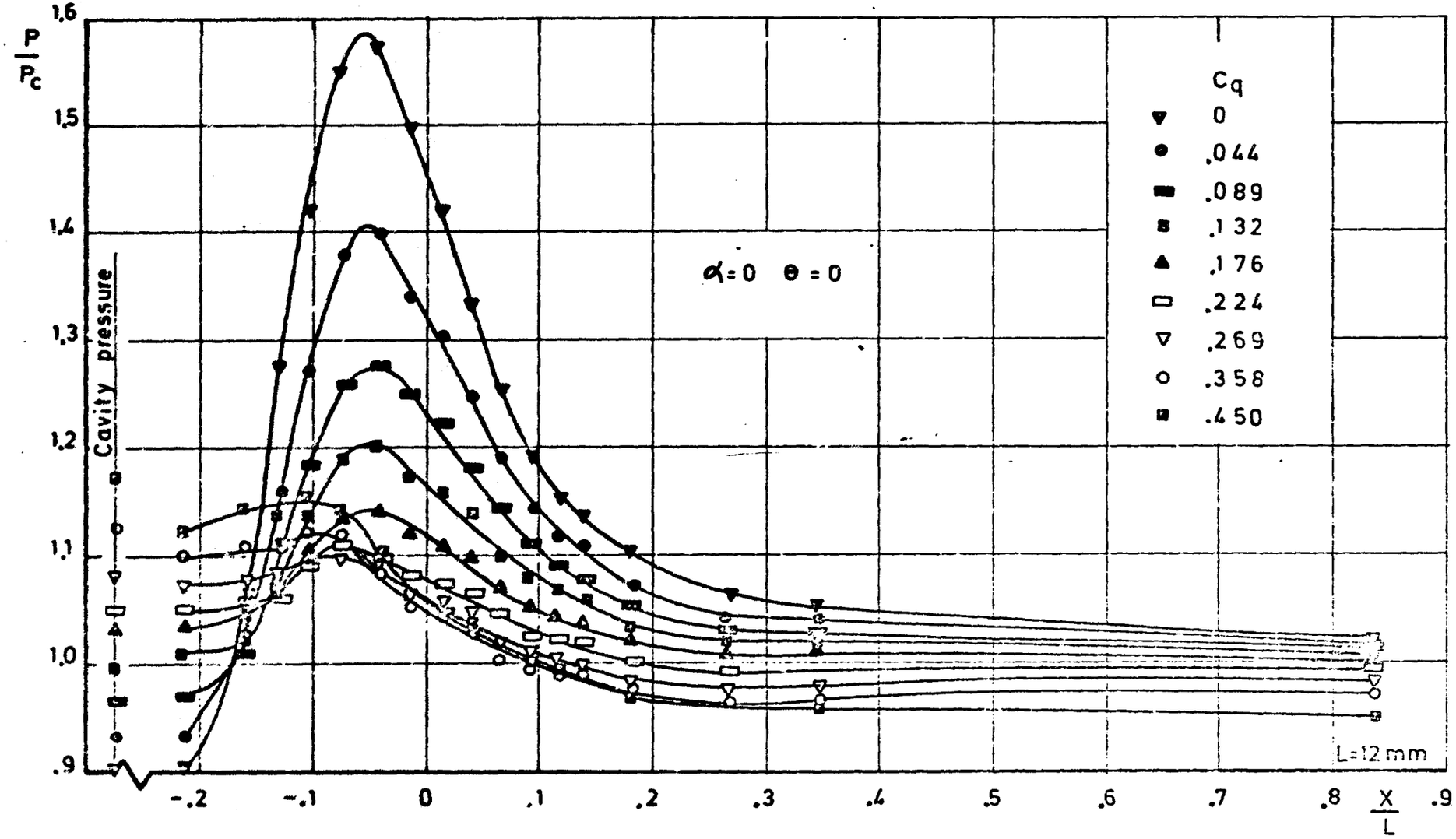

Fig. 2.1–PRESSURE DISTRIBUTIONS WITH AND WITHOUT AIR INJECTION

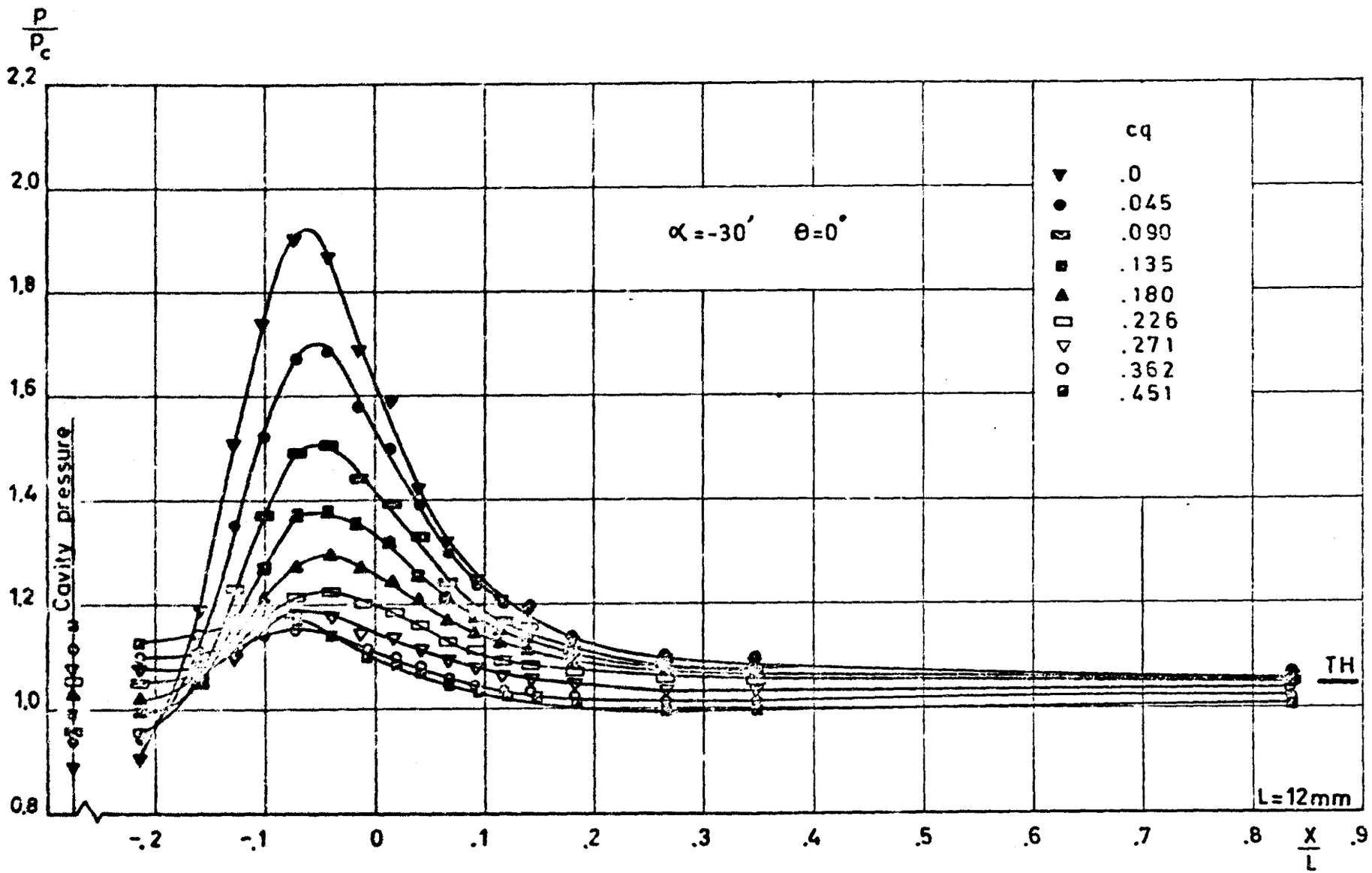

Fig. 2.2 - CONTINUED

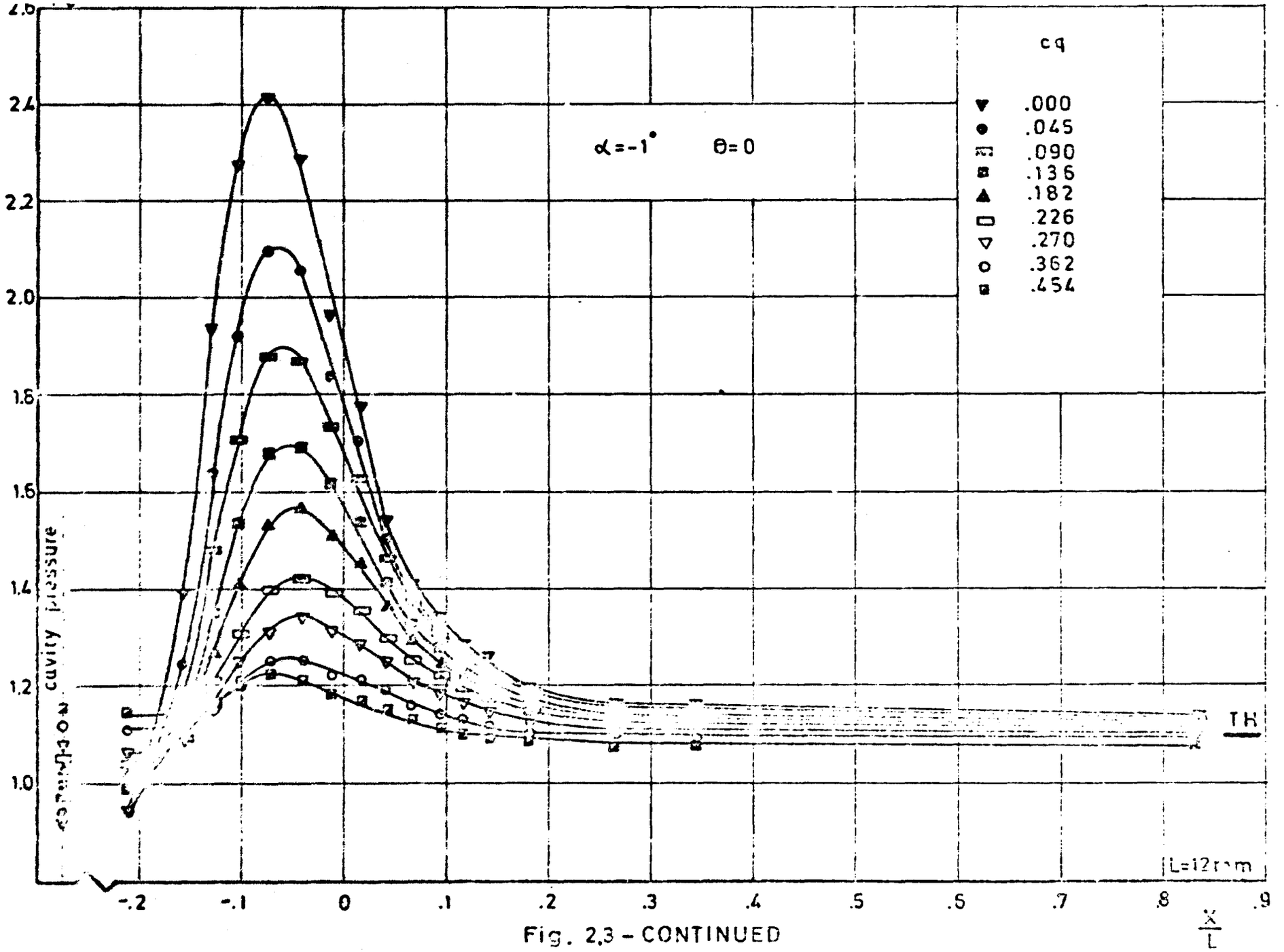

Fig. 2.3 – CONTINUED

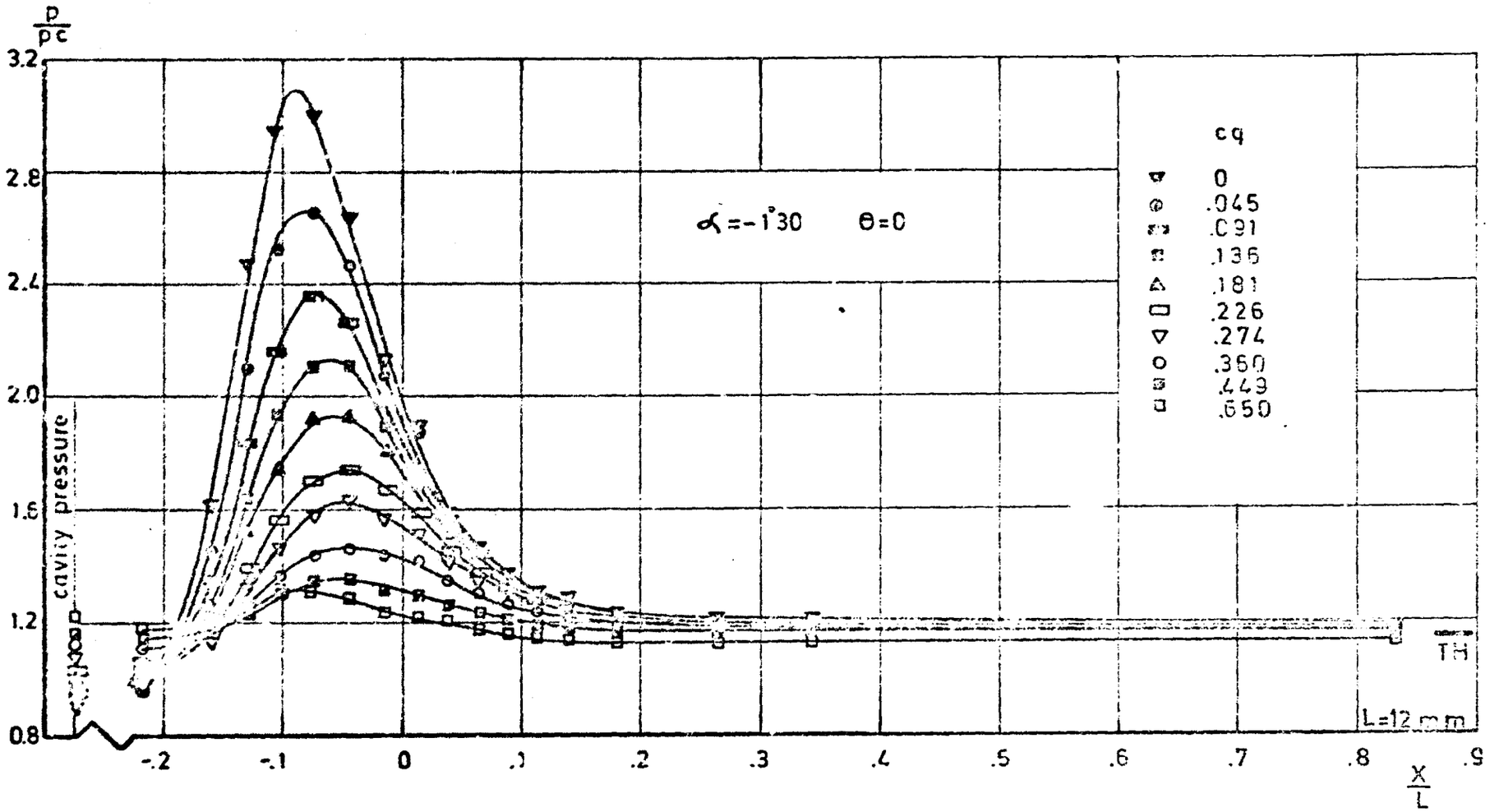

Fig. 24 – CONTINUED

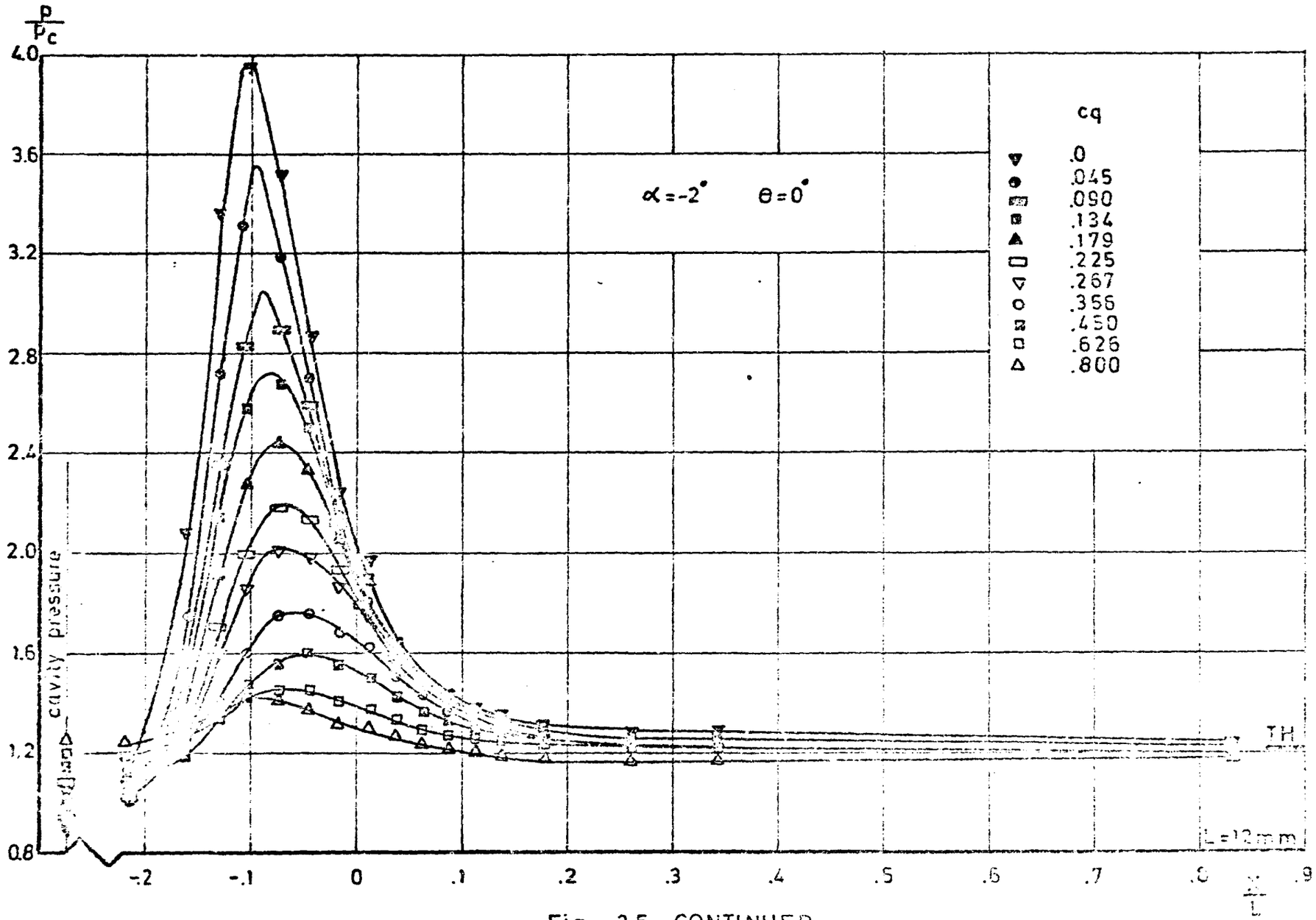

Fig. 2.5 - CONTINUED

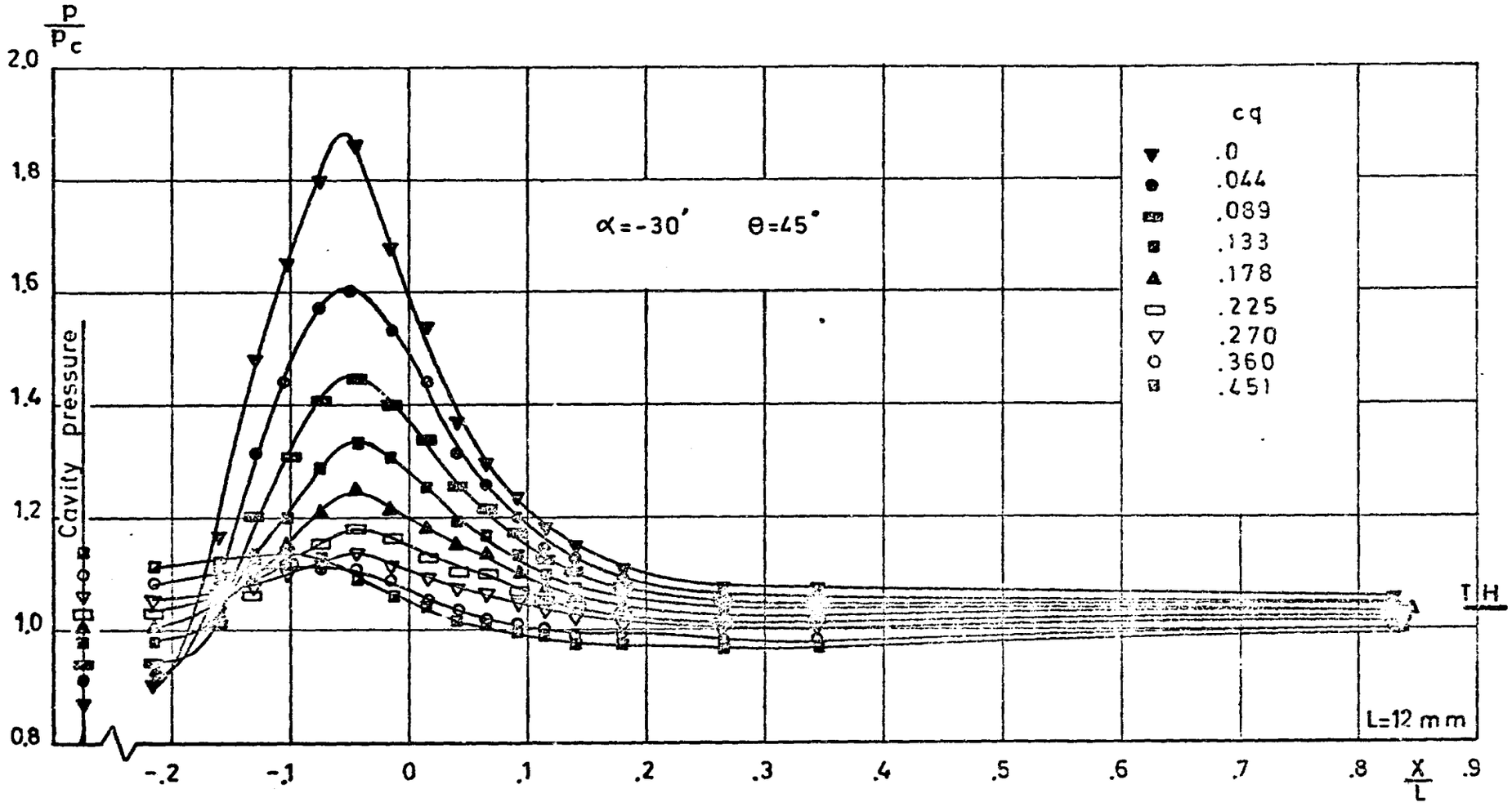

Fig. 2.6 — CONTINUED

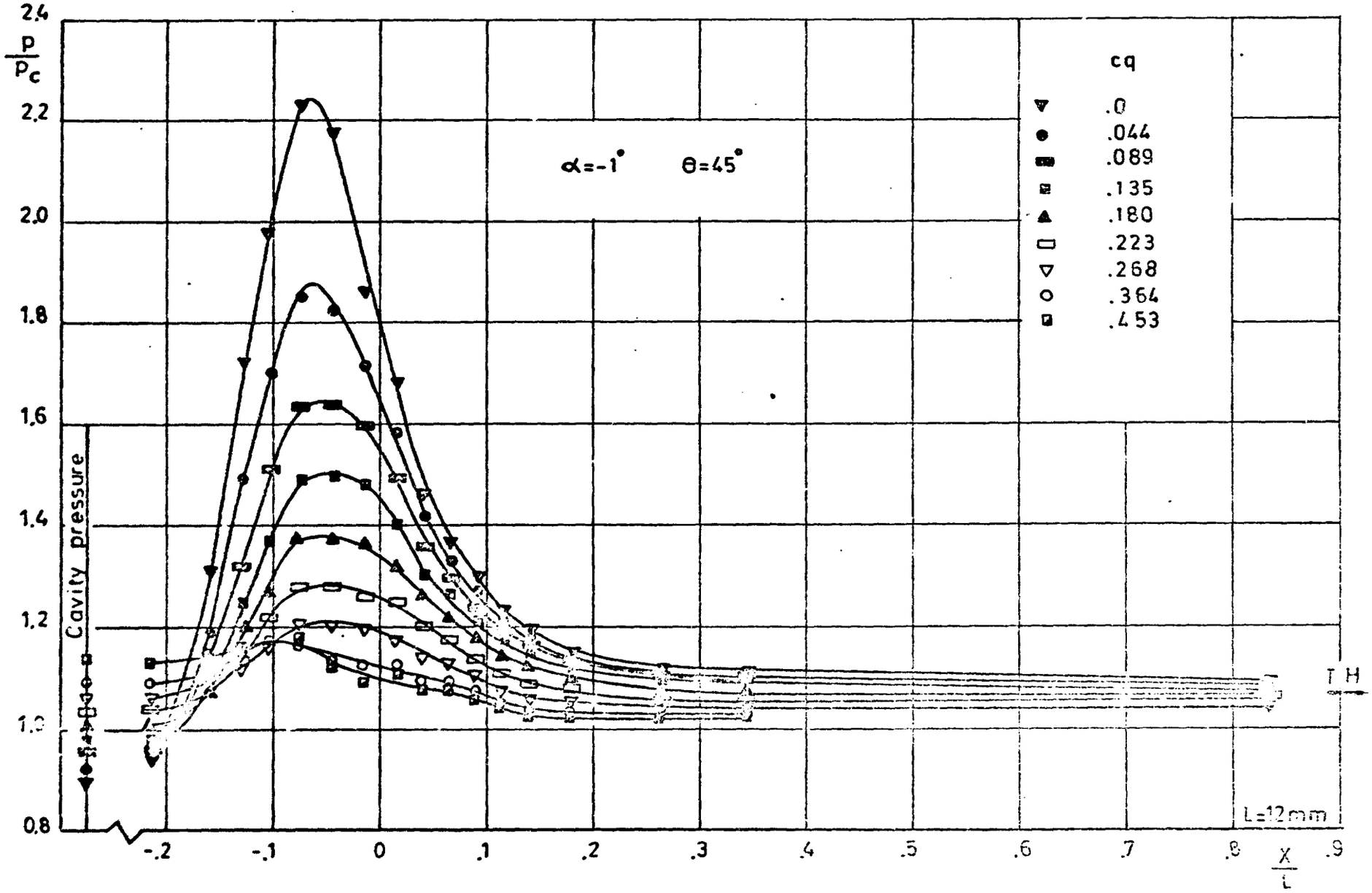

Fig. 2.7 - CONTINUED

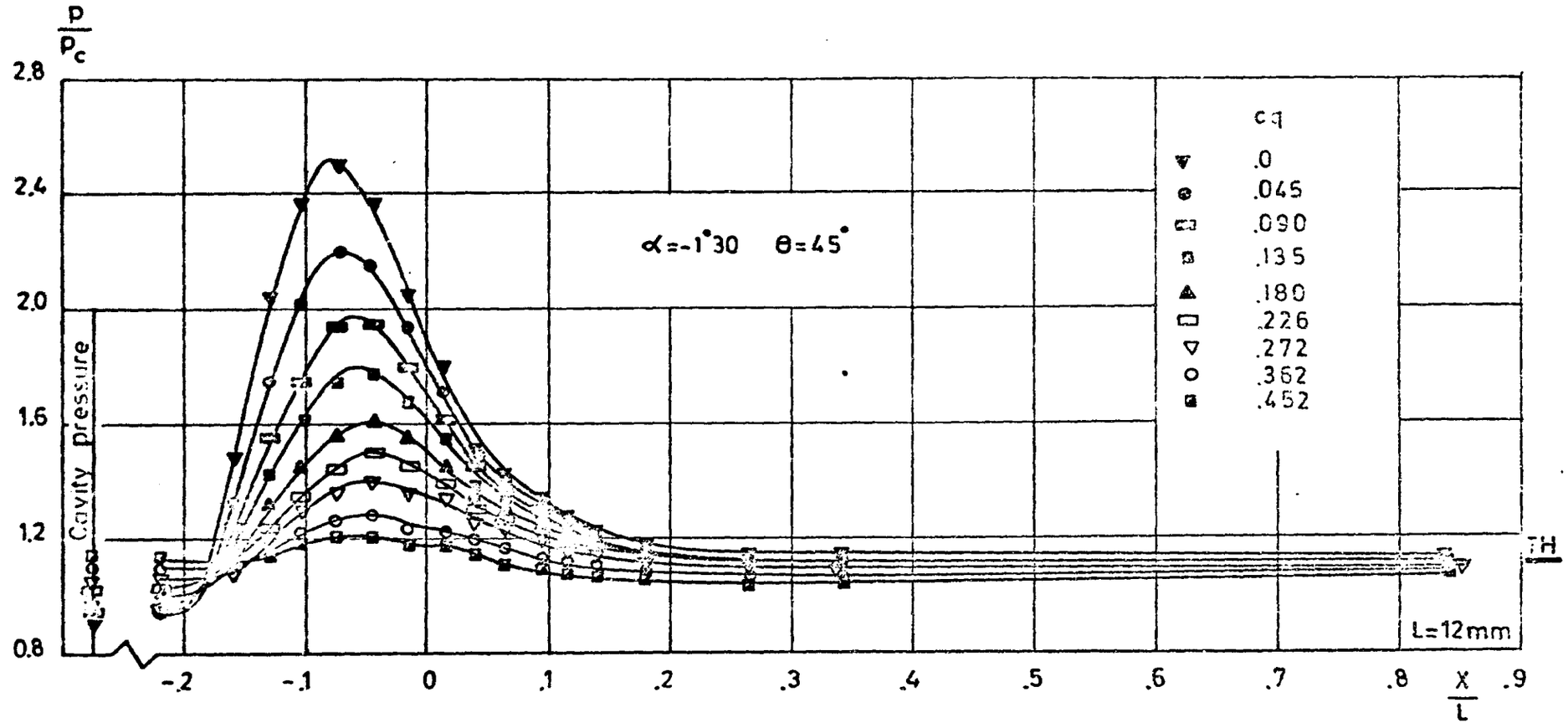

Fig . 2.8 — CONTINUED

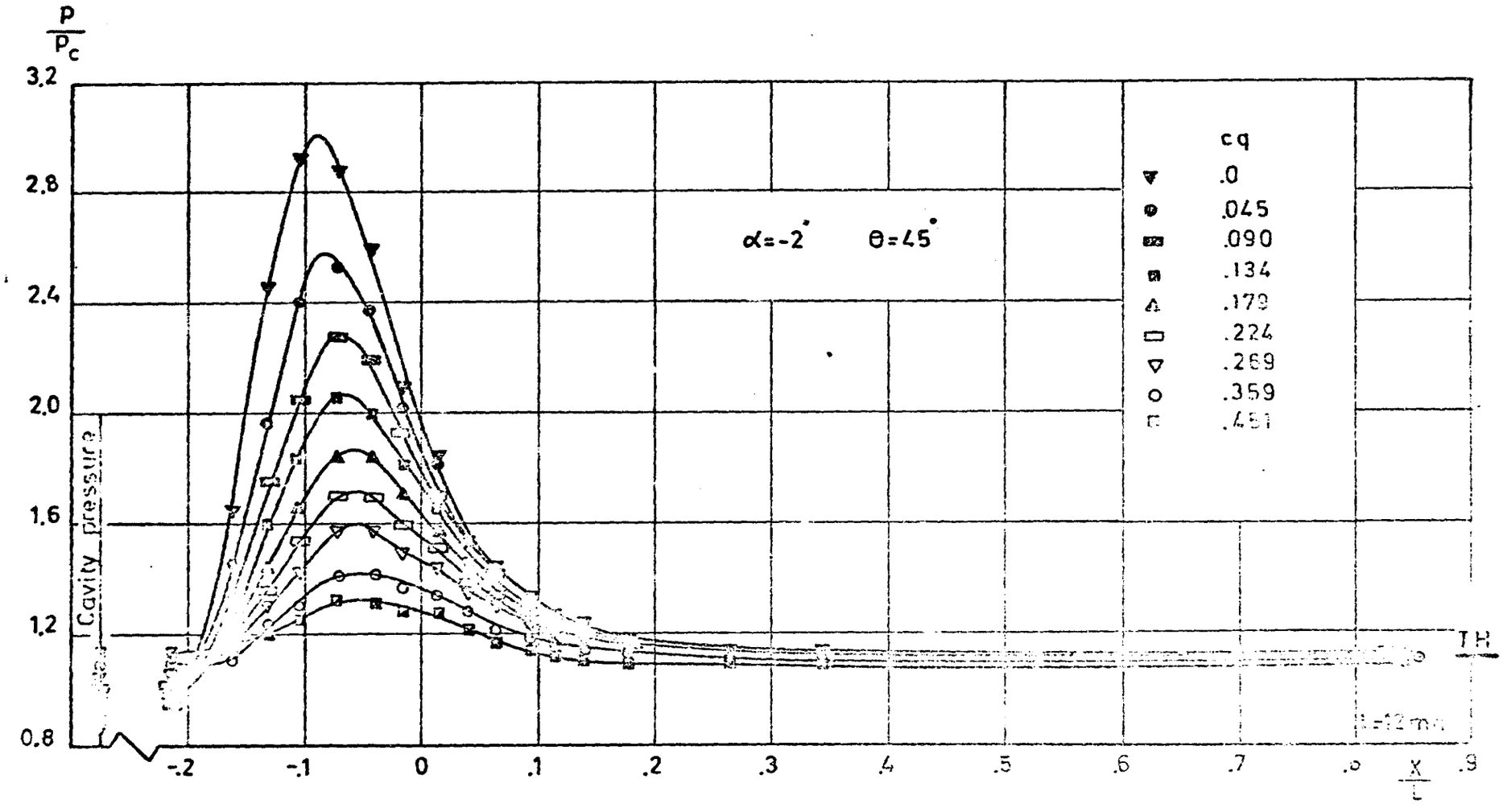

Fig. 2.9 – CONTINUED

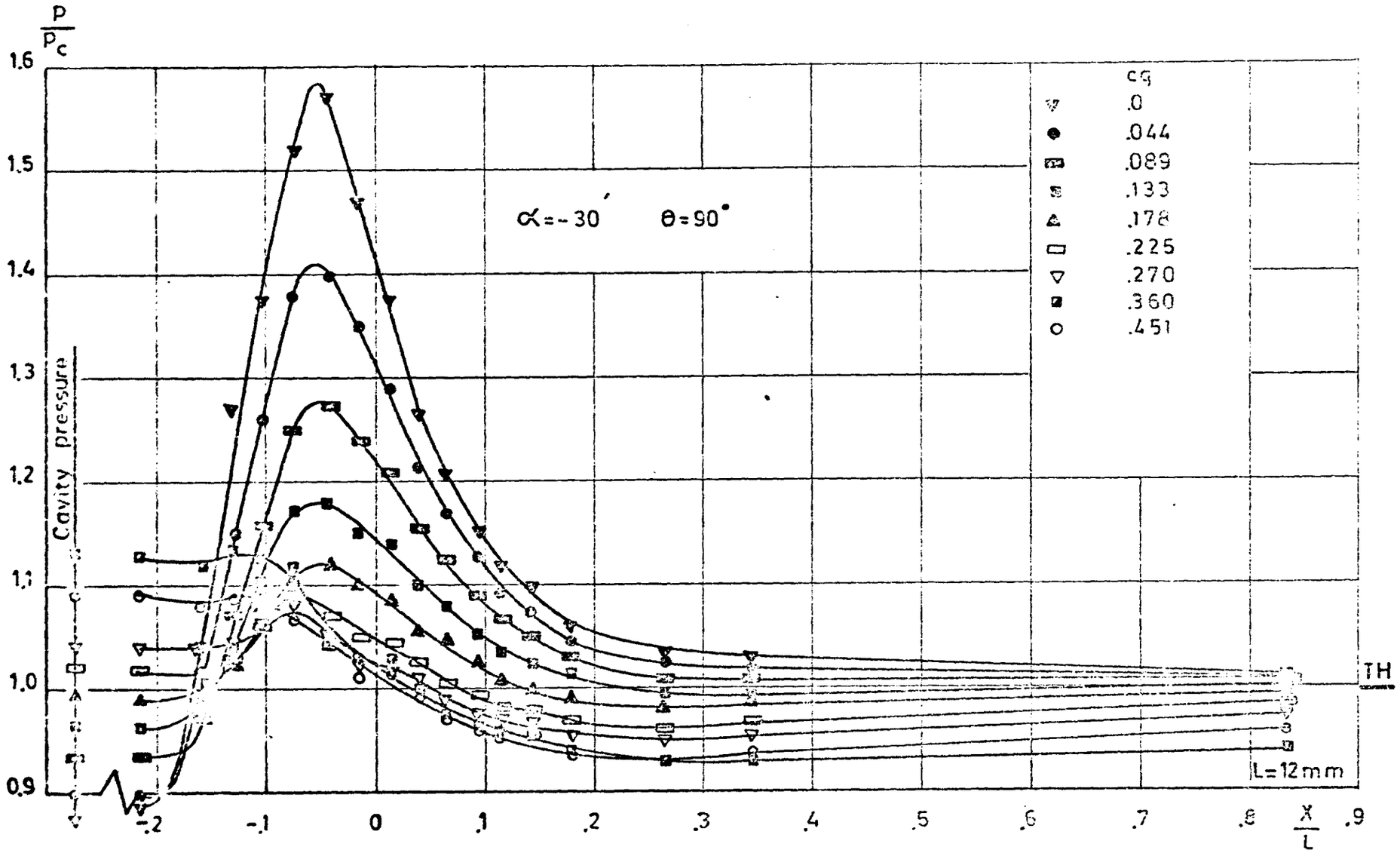

Fig. 2.10 – CONTINUED

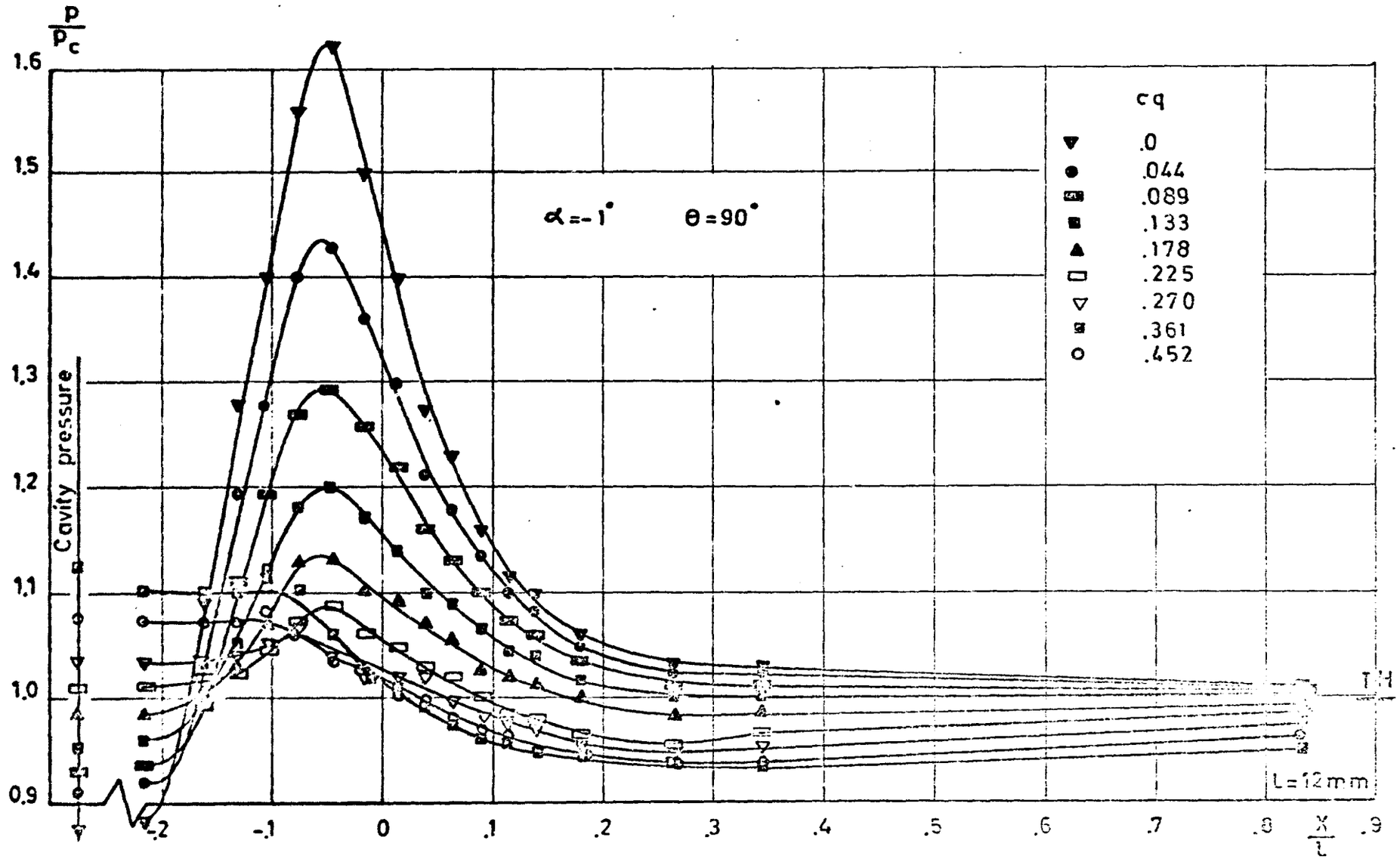

Fig. 2.11 - CONTINUED

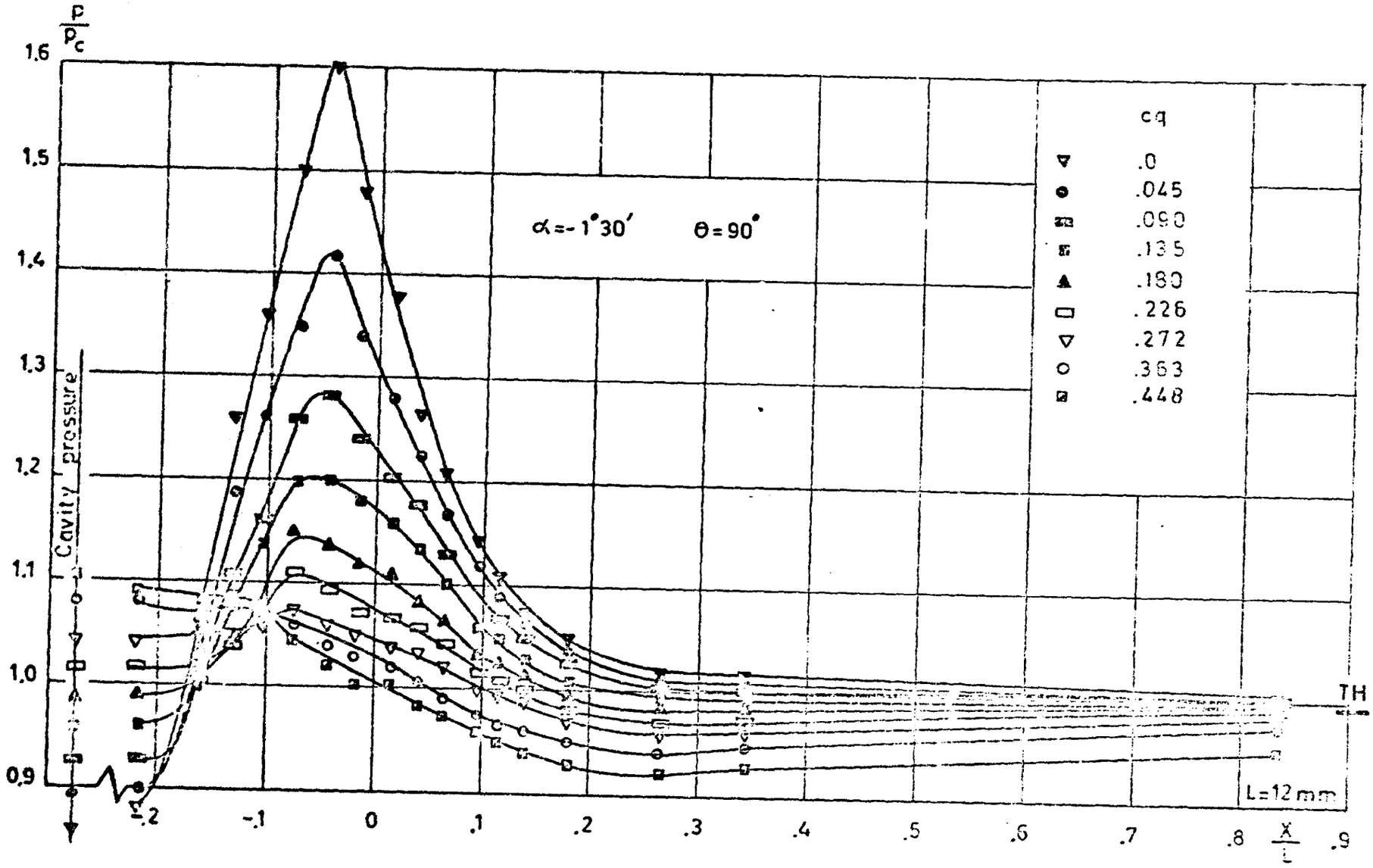

Fig. 2.12 - CONTINUED

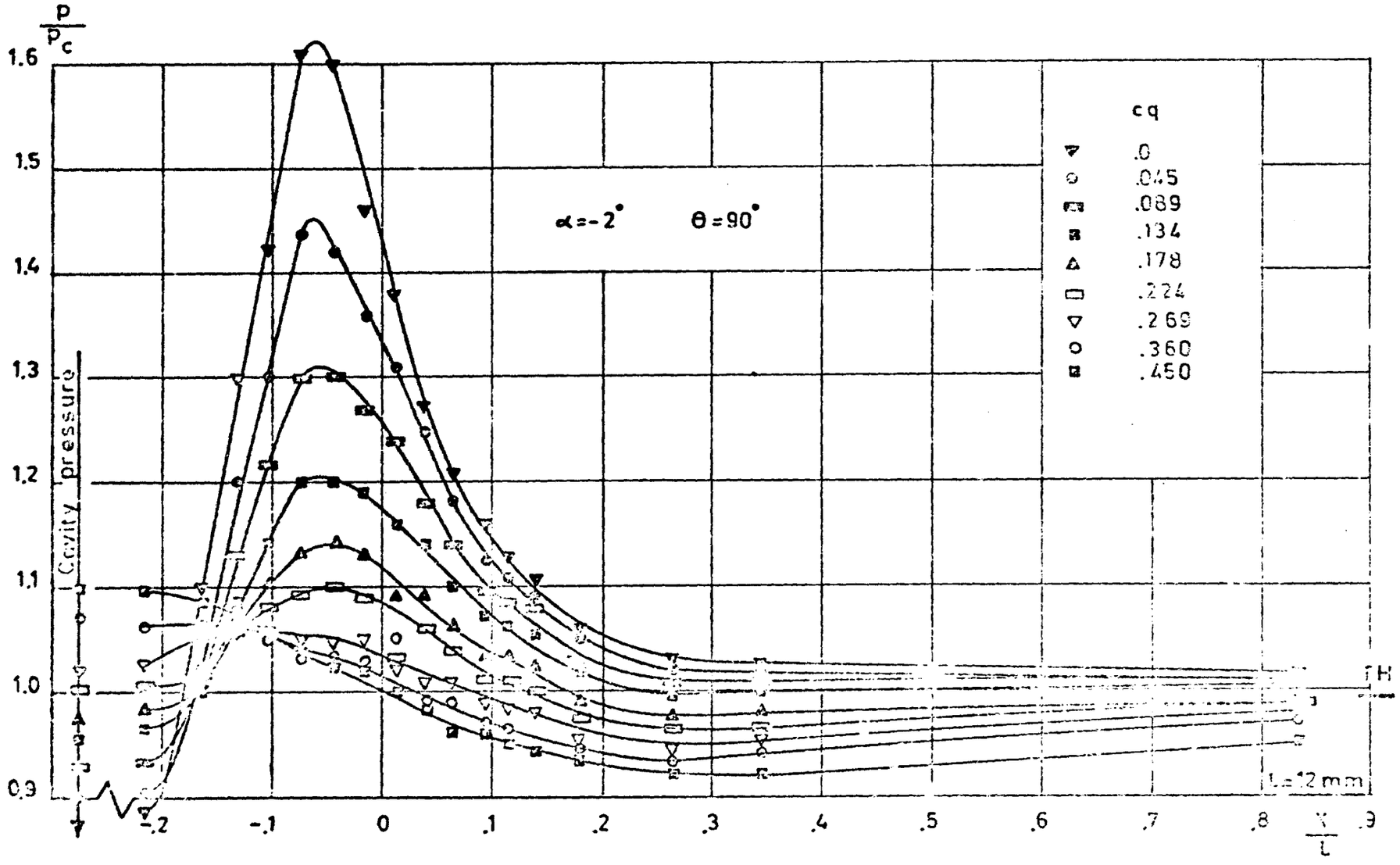

Fig. 2.13 - CONTINUED

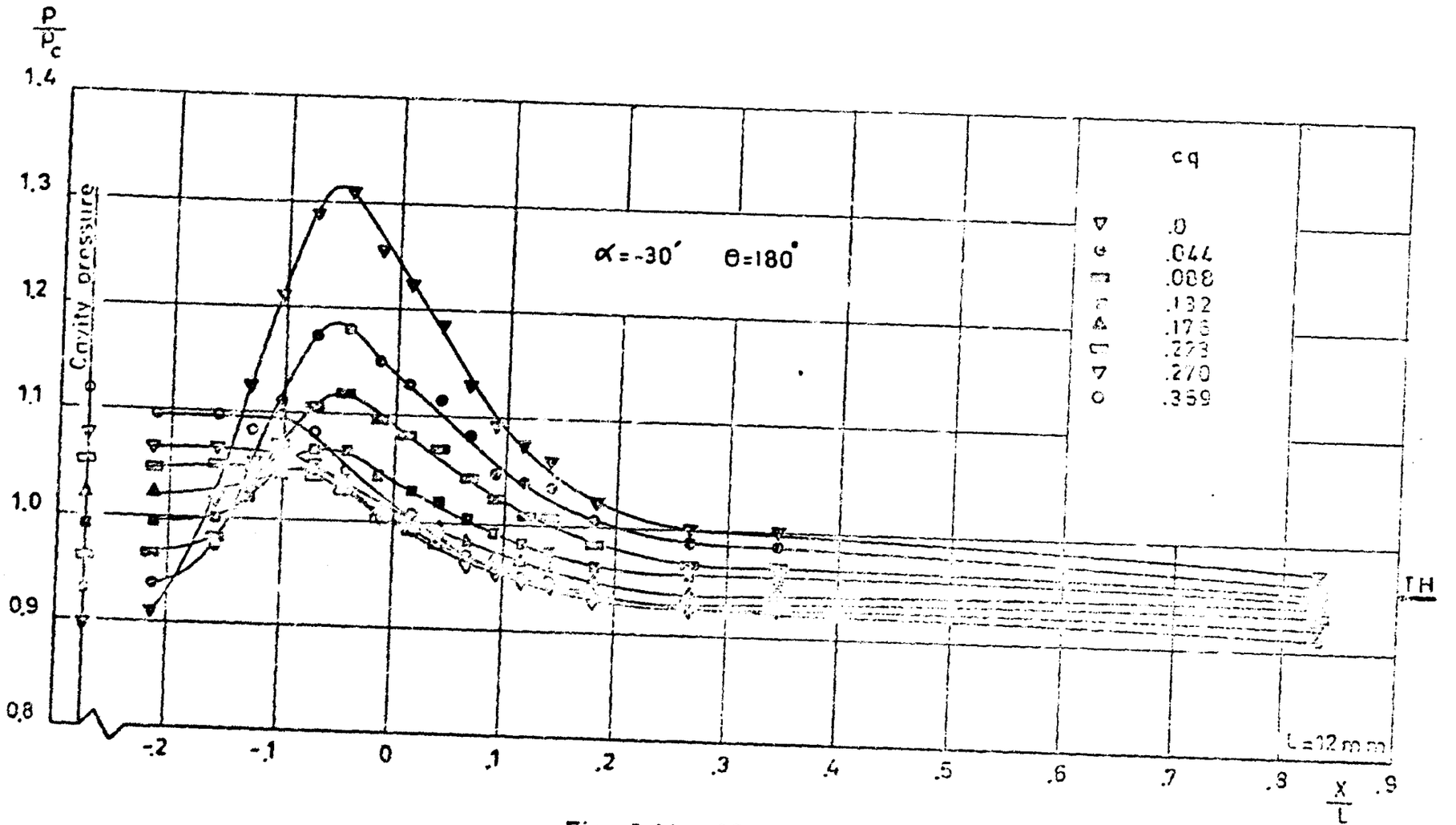

Fig. 2.14 - CONTINUED

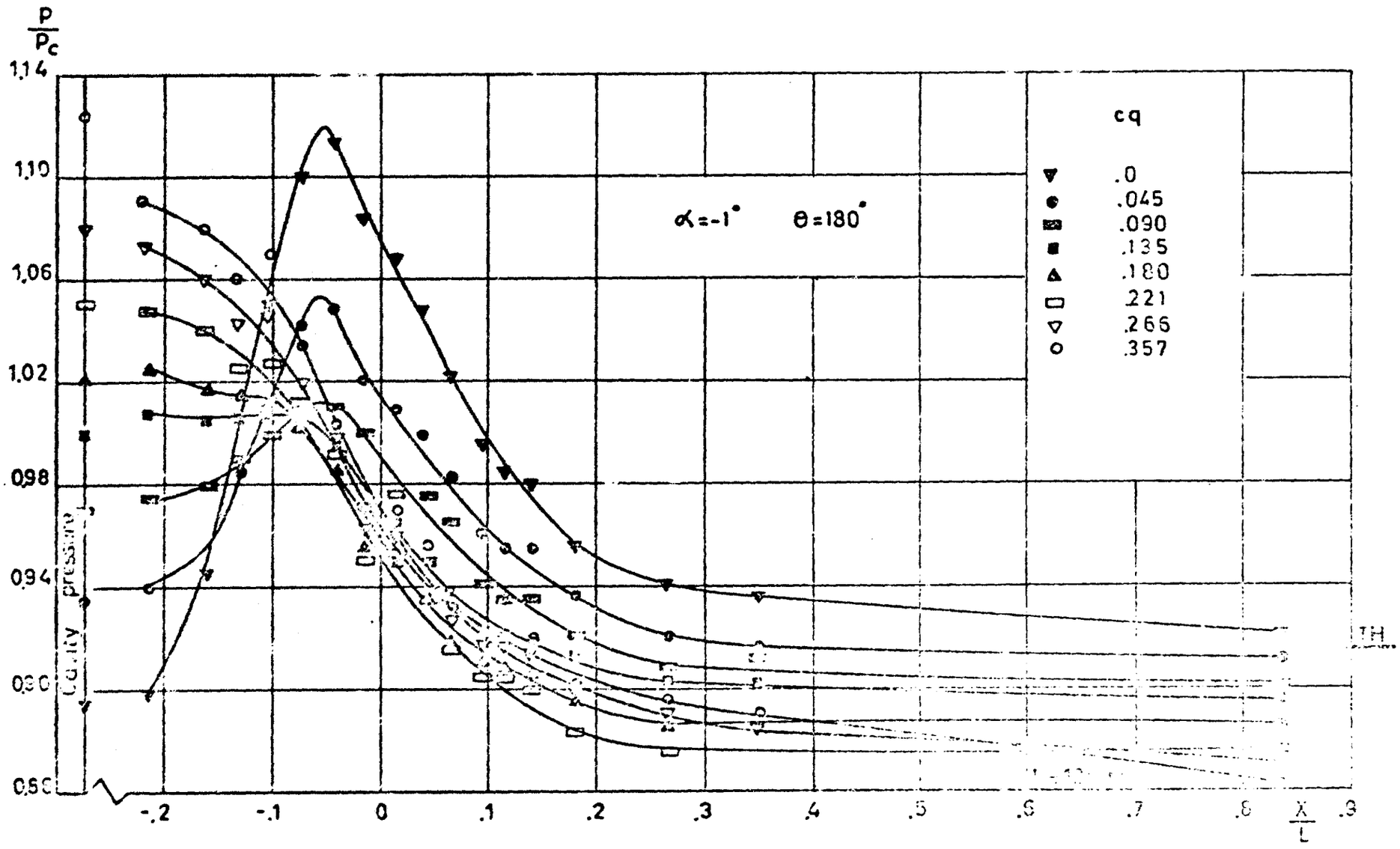

Fig. 2.15 – CONTINUED

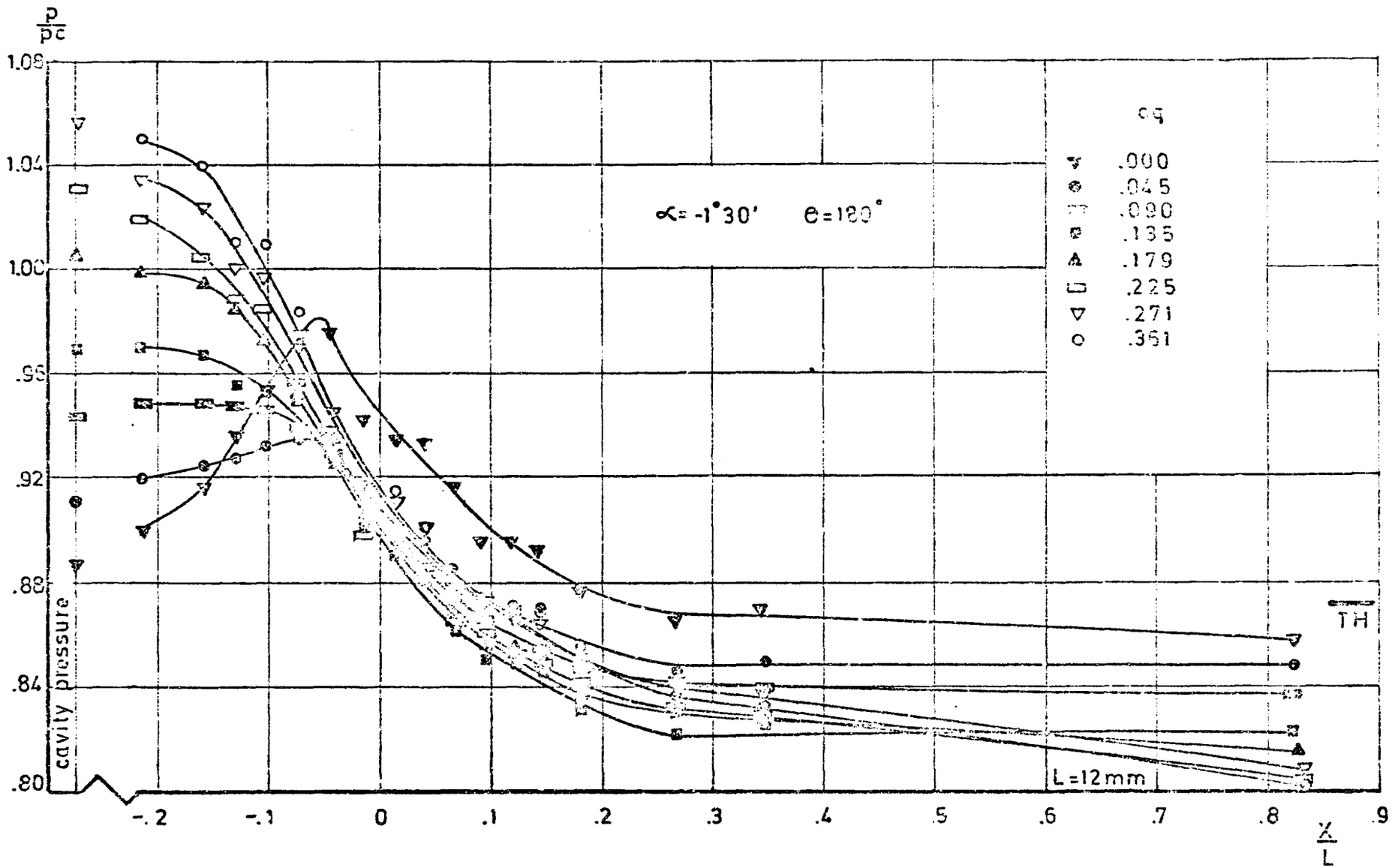

Fig. 2.16 – CONTINUED

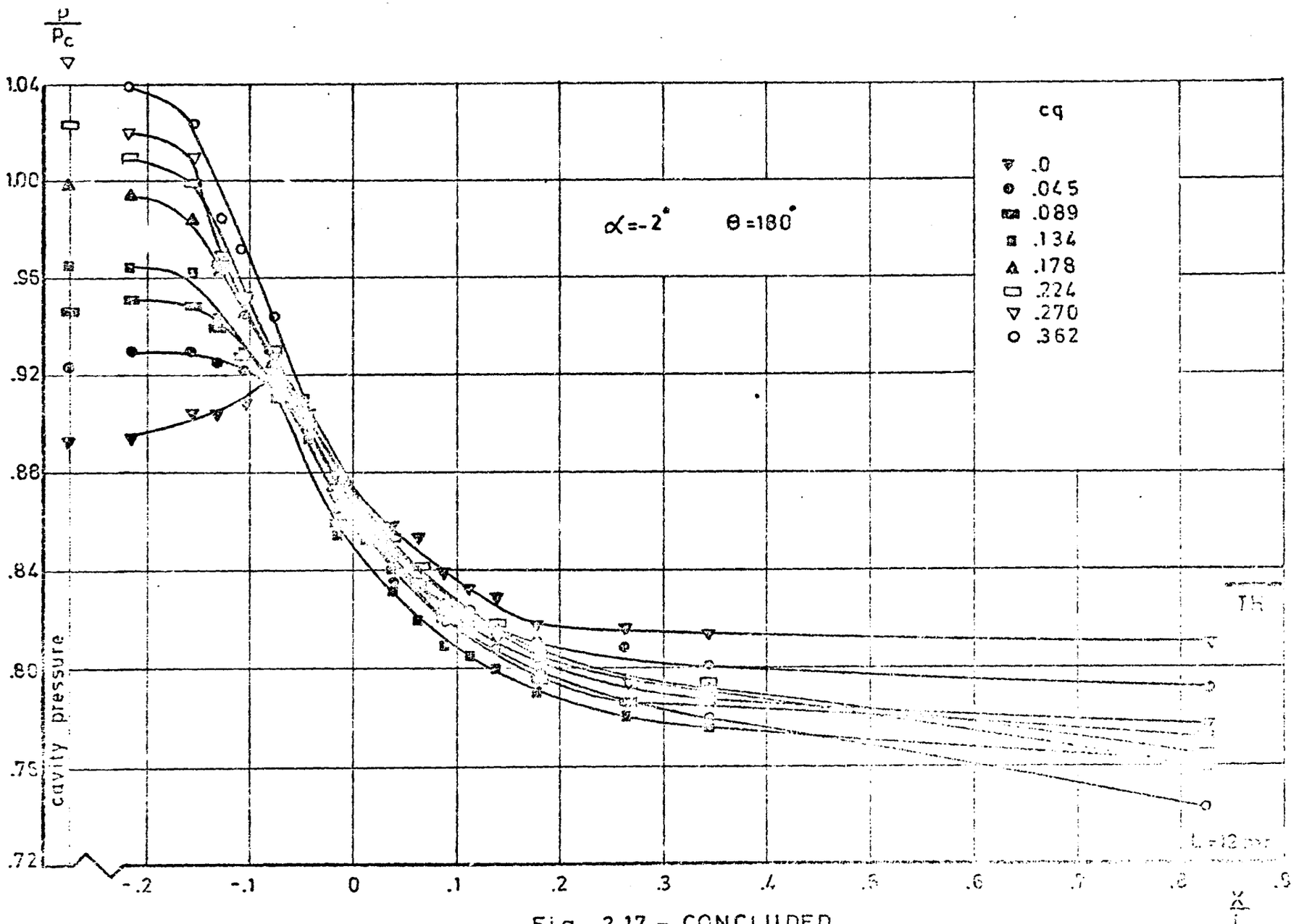

Fig. 2.17 - CONCLUDED

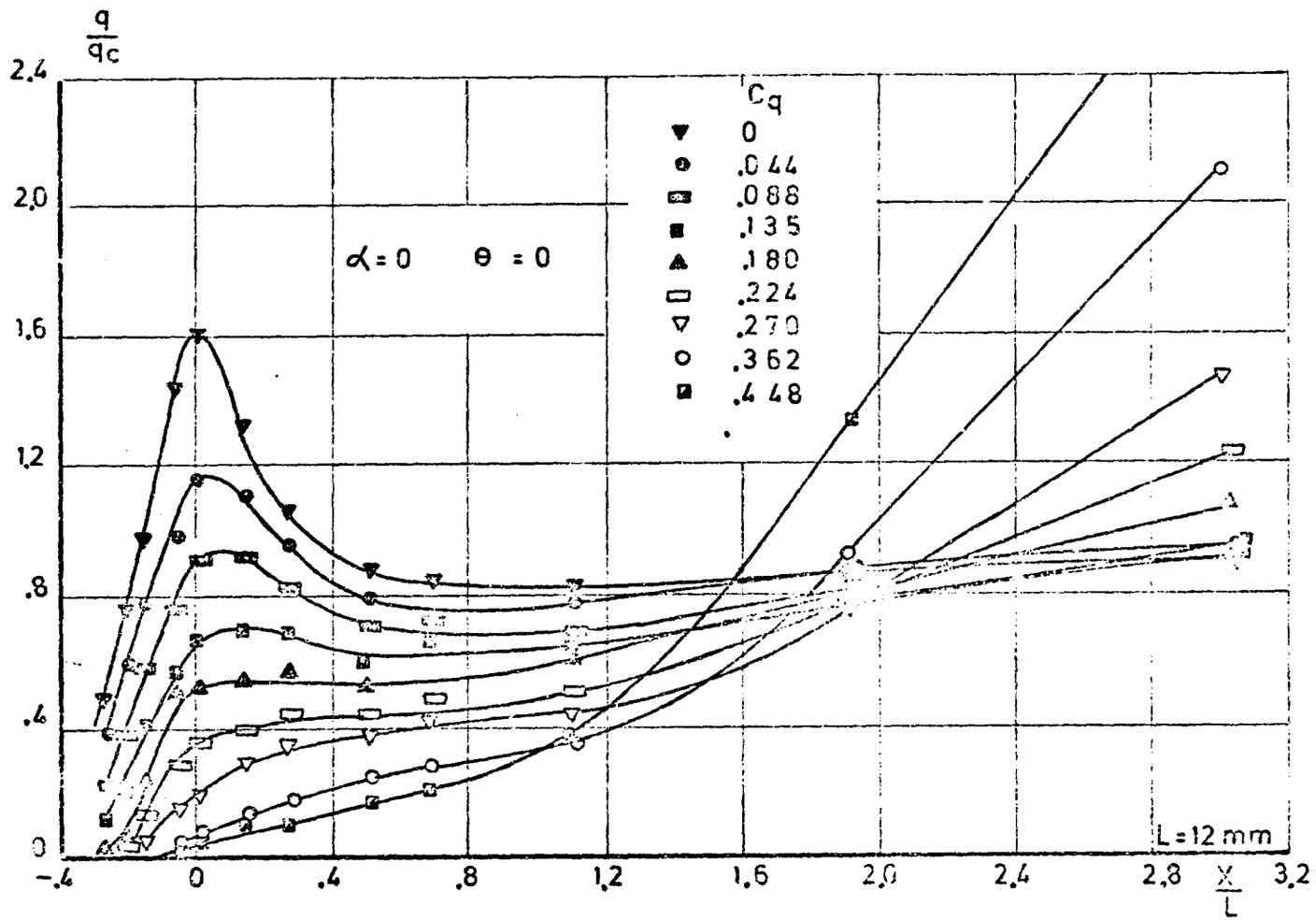

Fig. 3.1 – HEAT TRANSFER DISTRIBUTION WITH AND WITHOUT AIR INJECTION

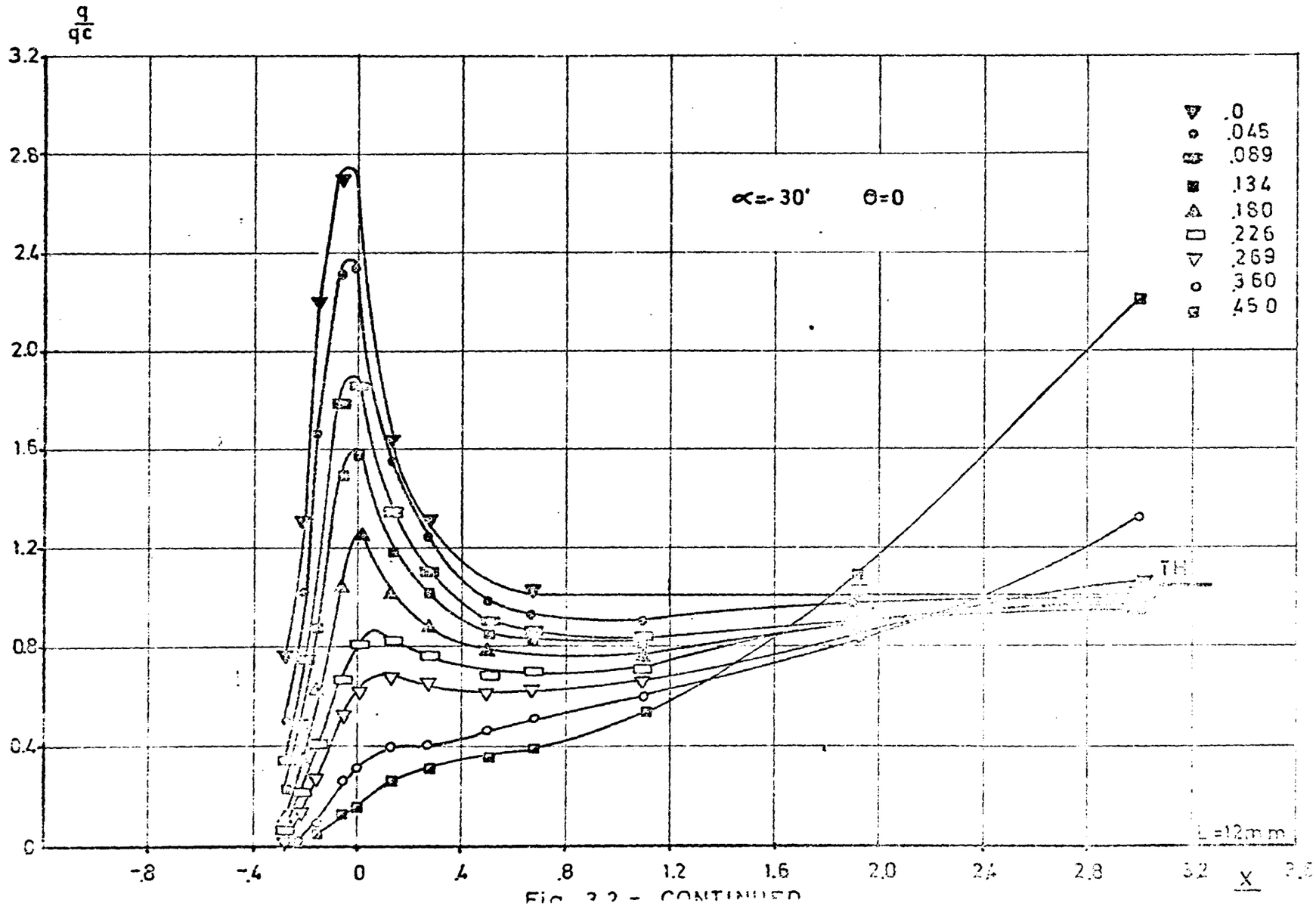

Fig. 3.2 - CONTINUED

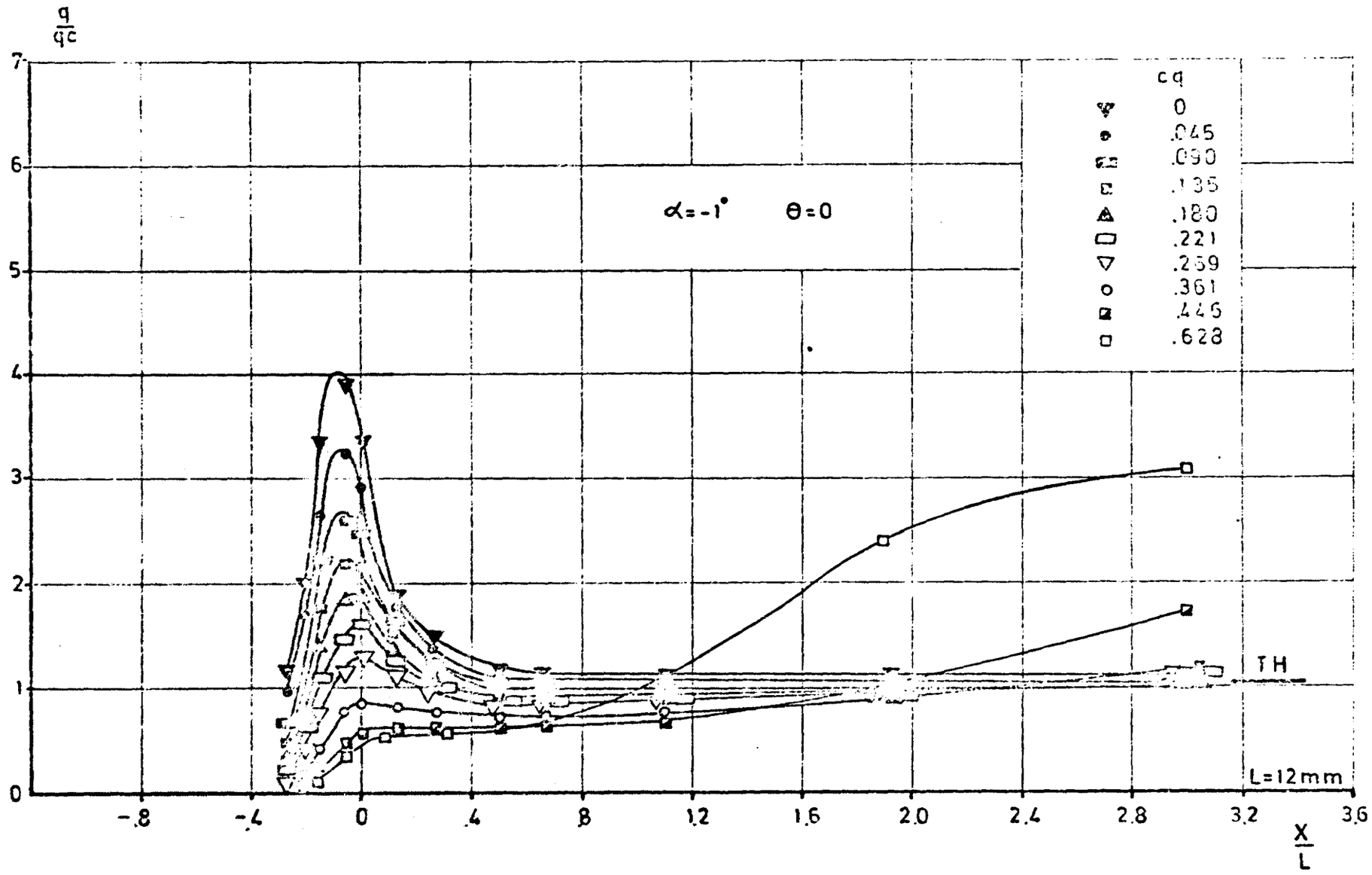

Fig. 3.3 - CONTINUED

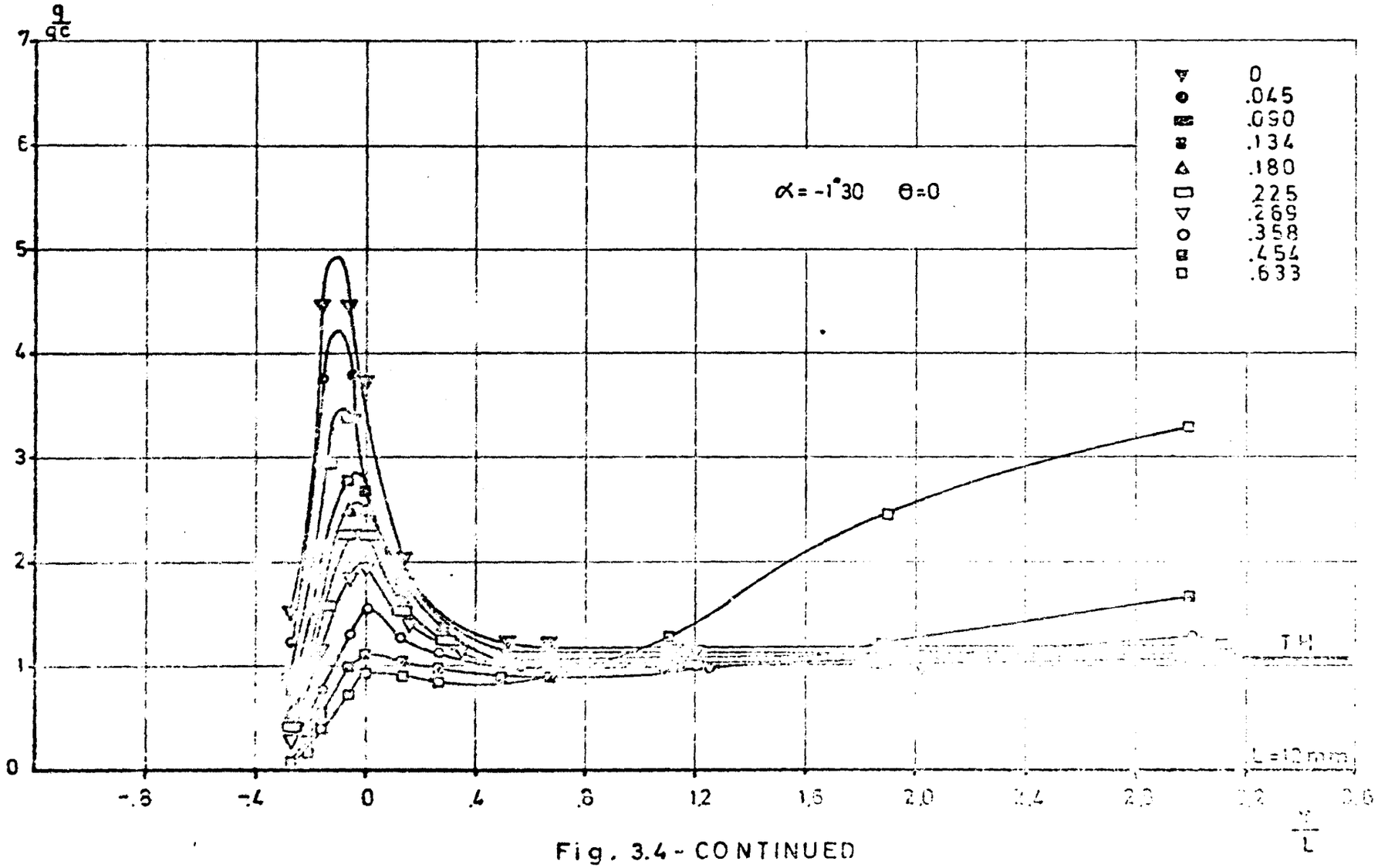

Fig. 3.4 - CONTINUED

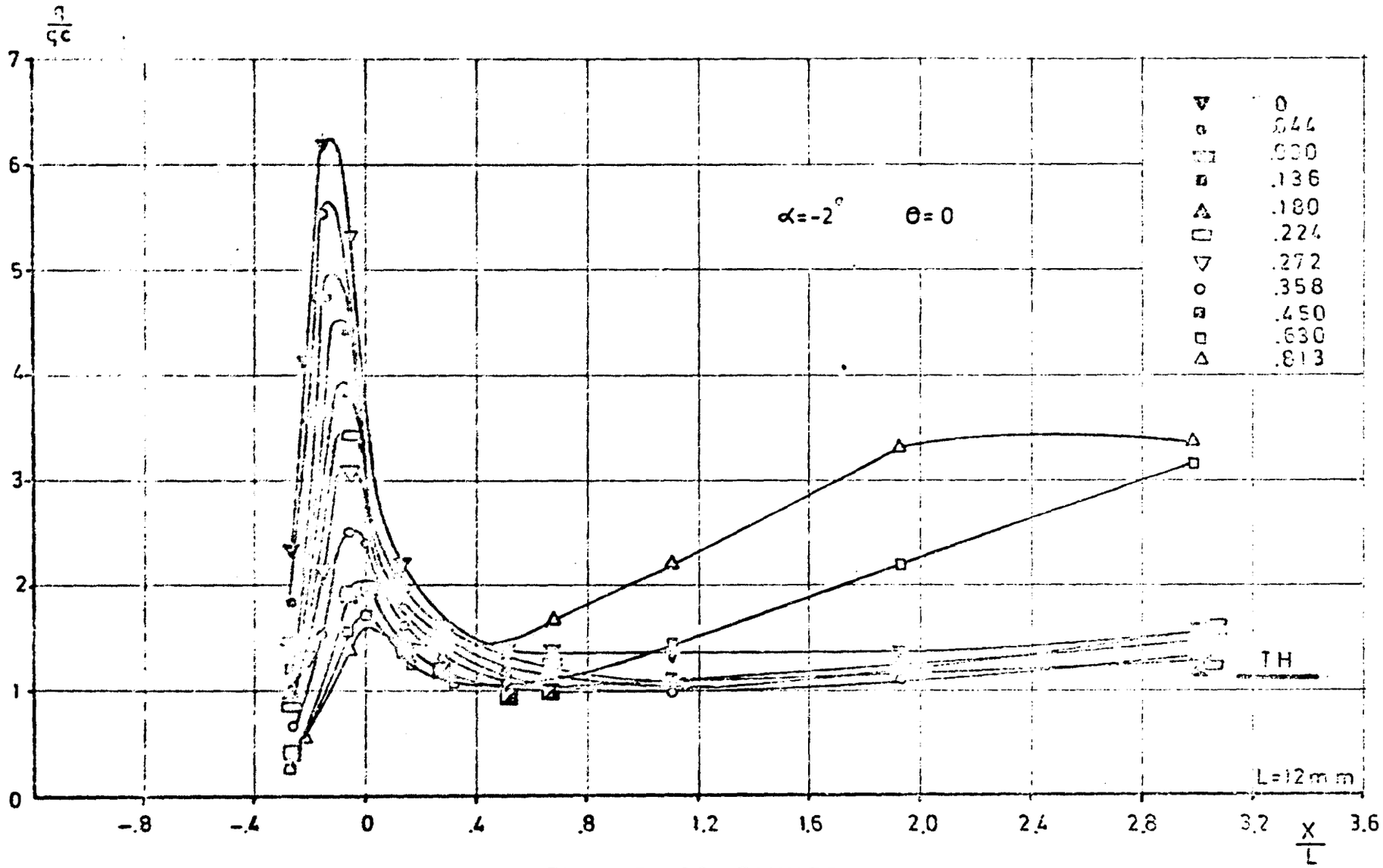

Fig. 3.5 - CONTINUED

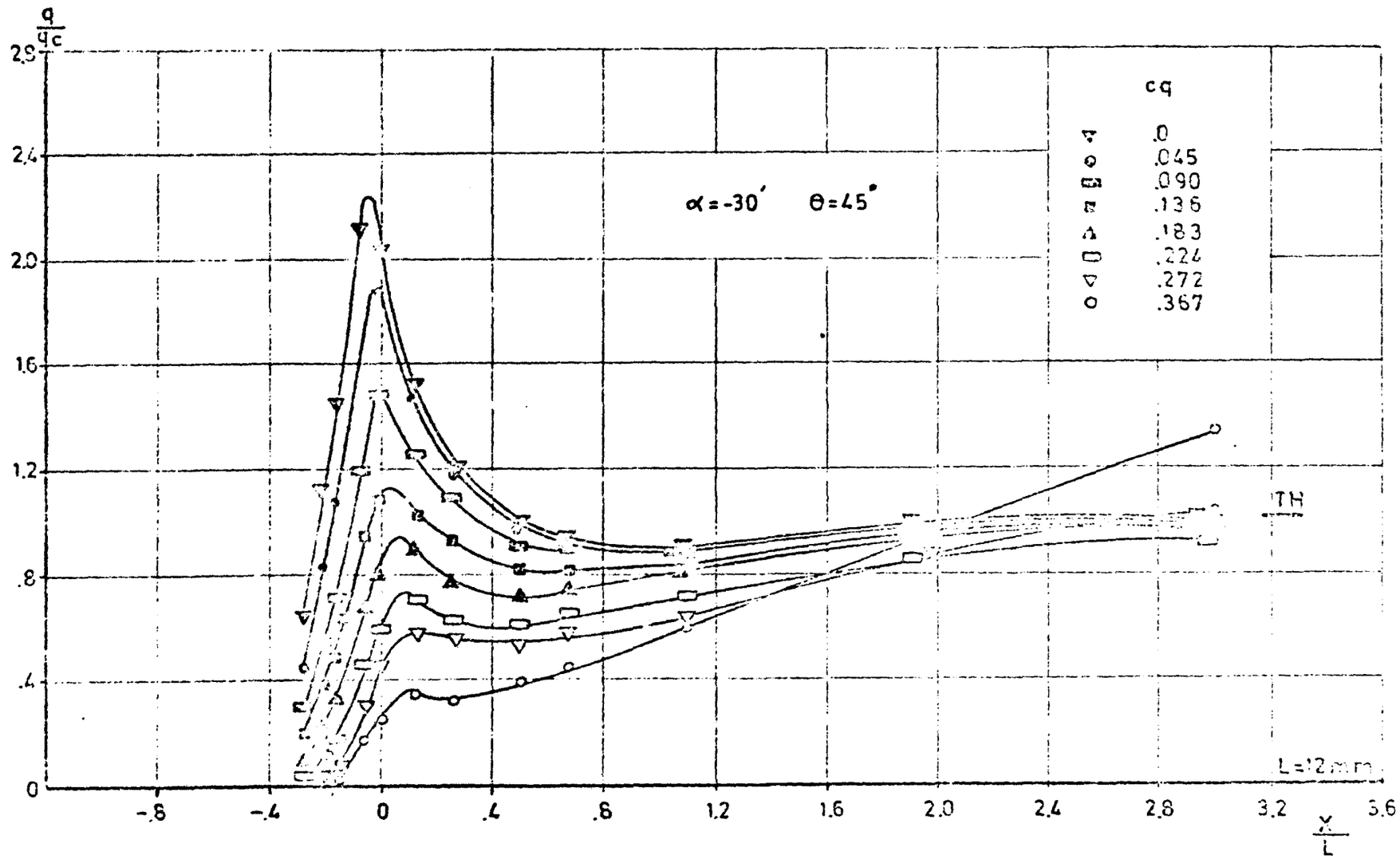

Fig. 3.6 - CONTINUED

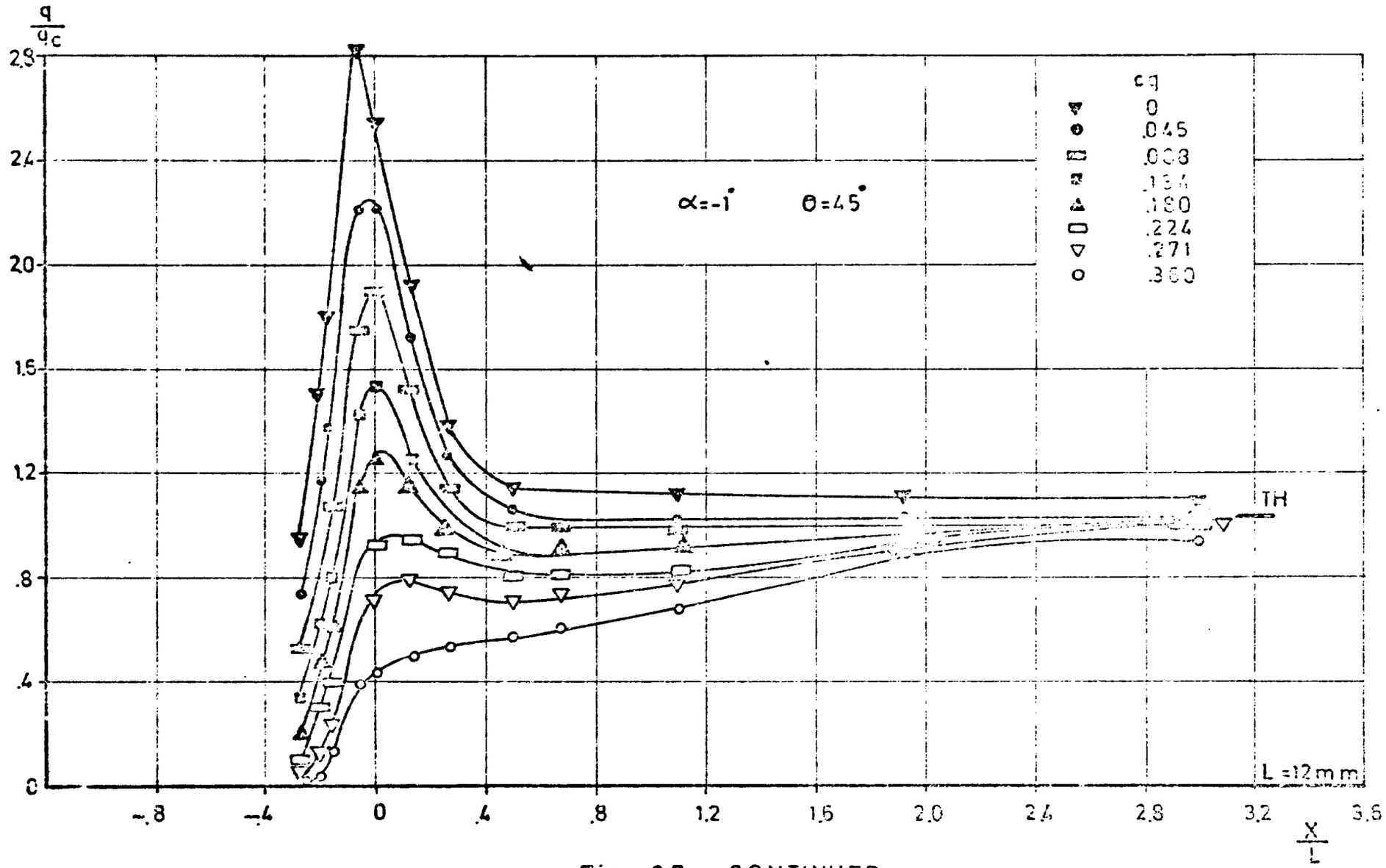

Fig. 3.7 - CONTINUED

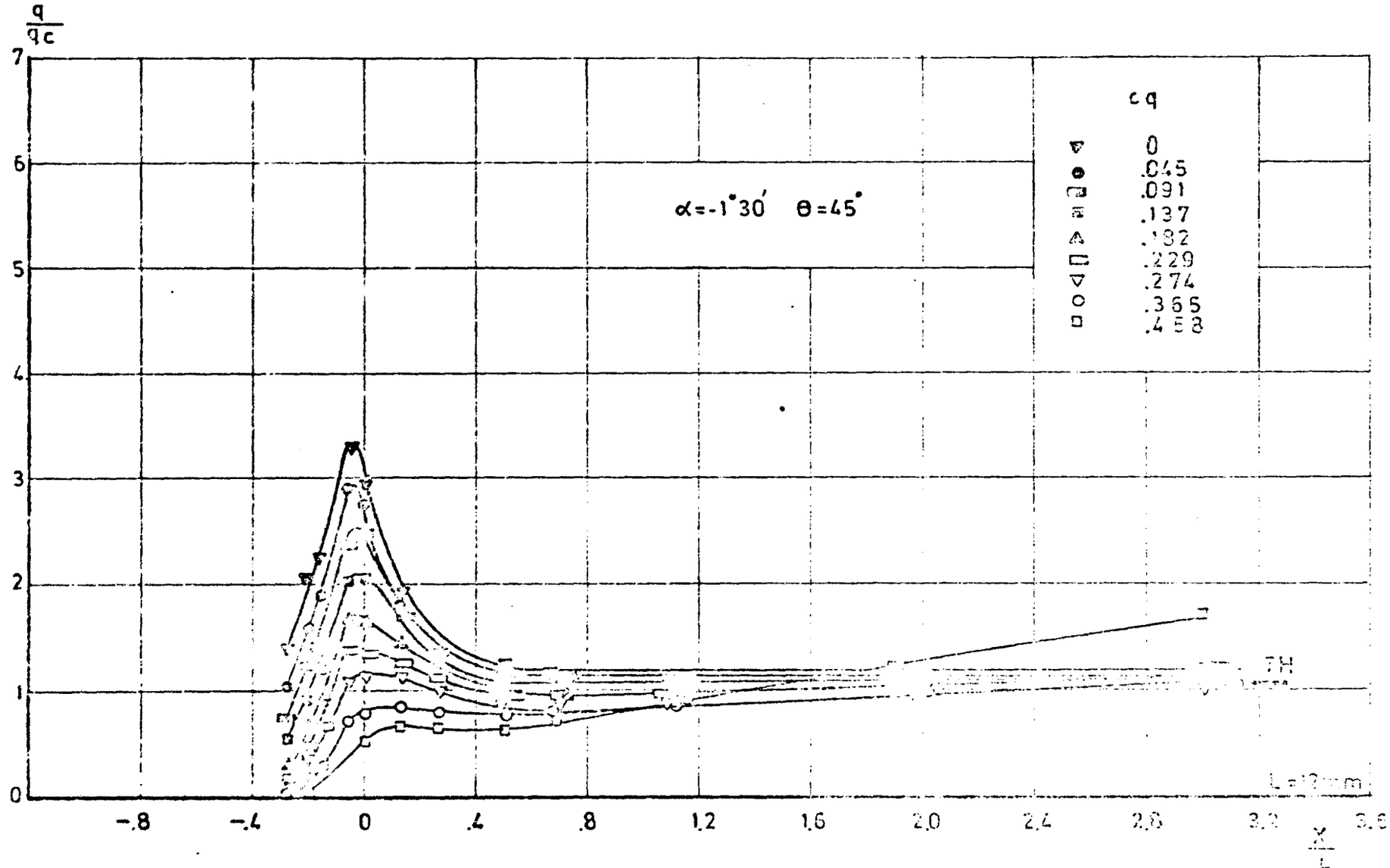

Fig. 3.8 - CONTINUED

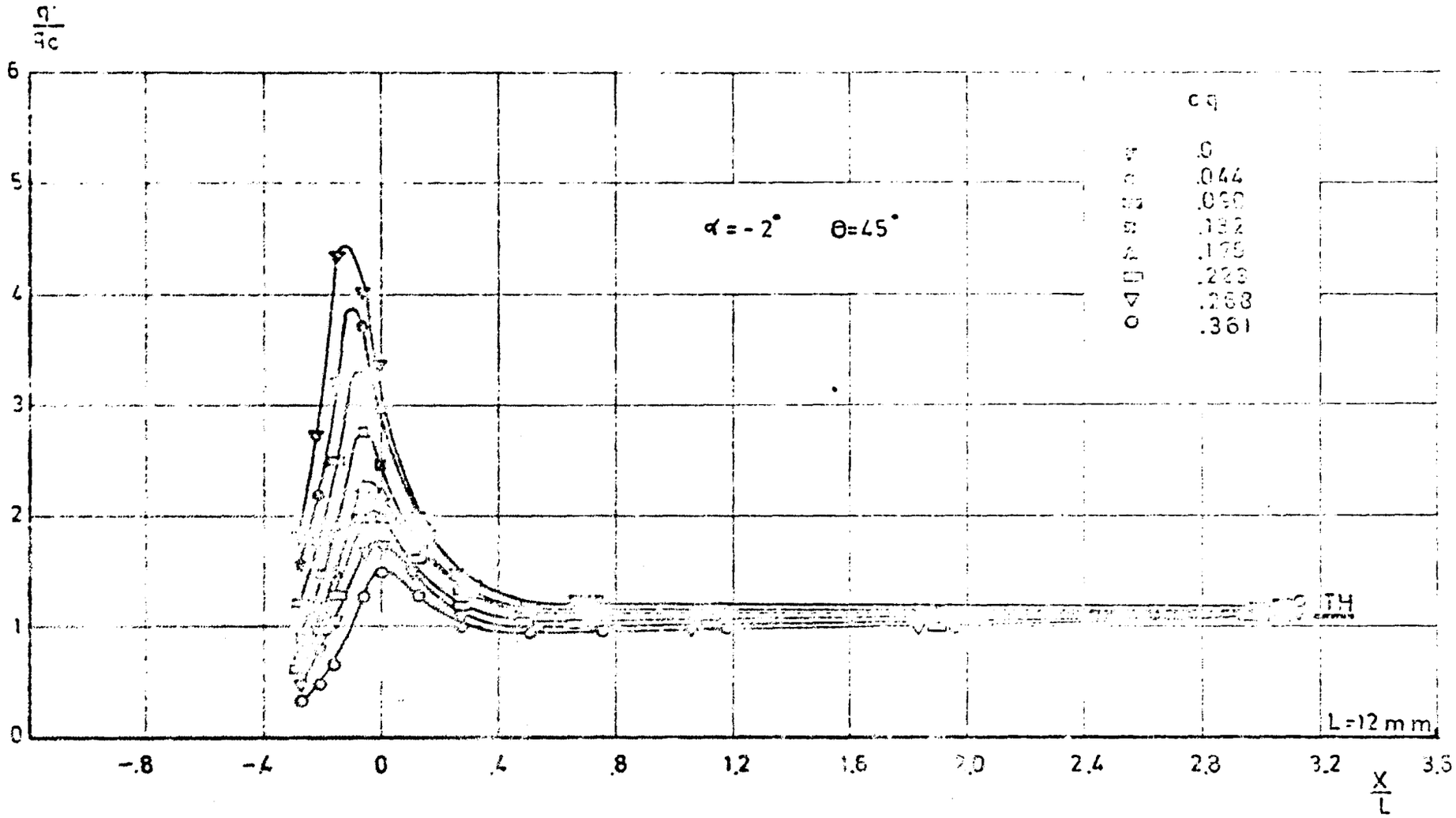

Fig. 3.9 - CONTINUED

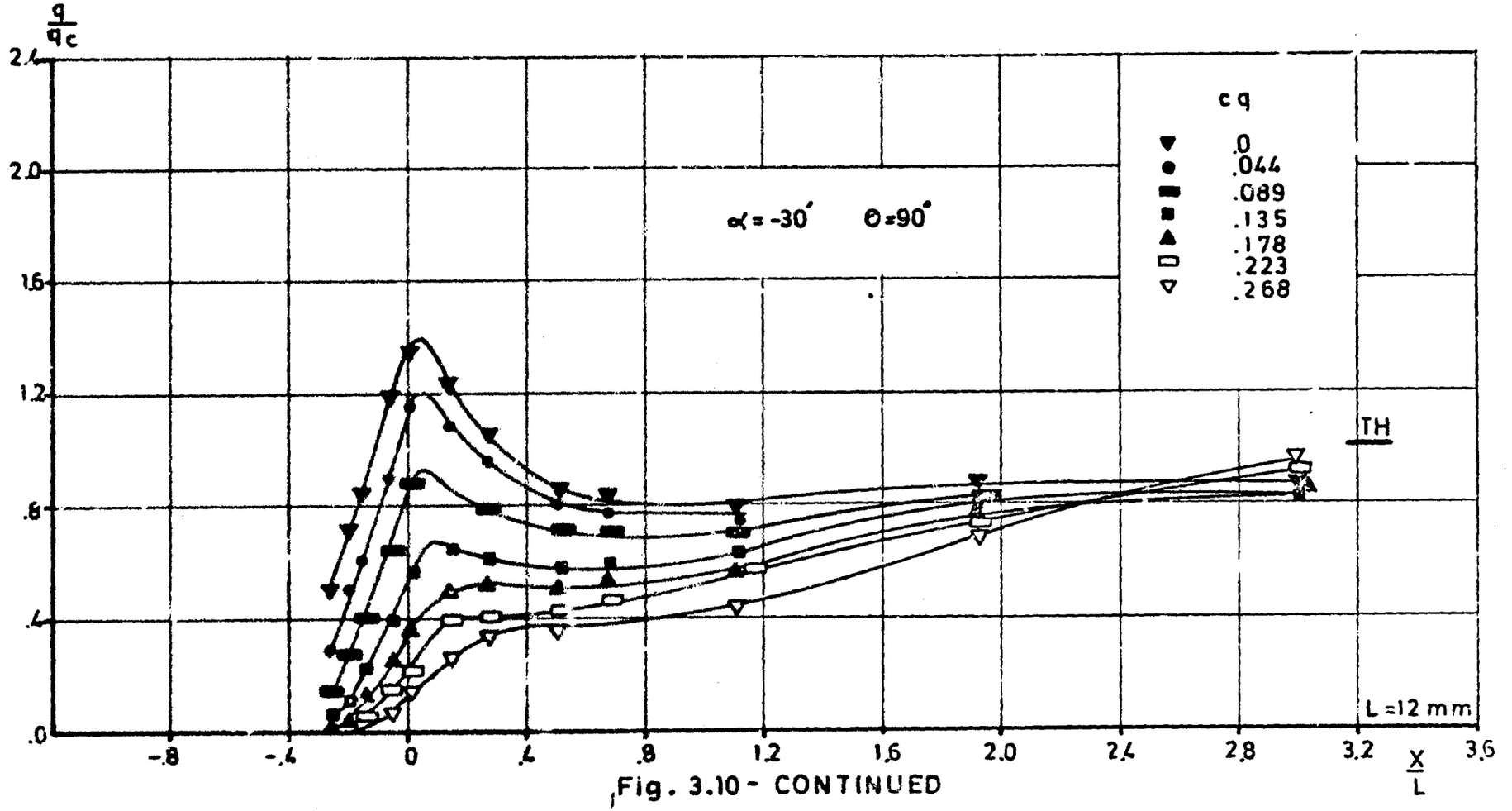

Fig. 3.10 - CONTINUED

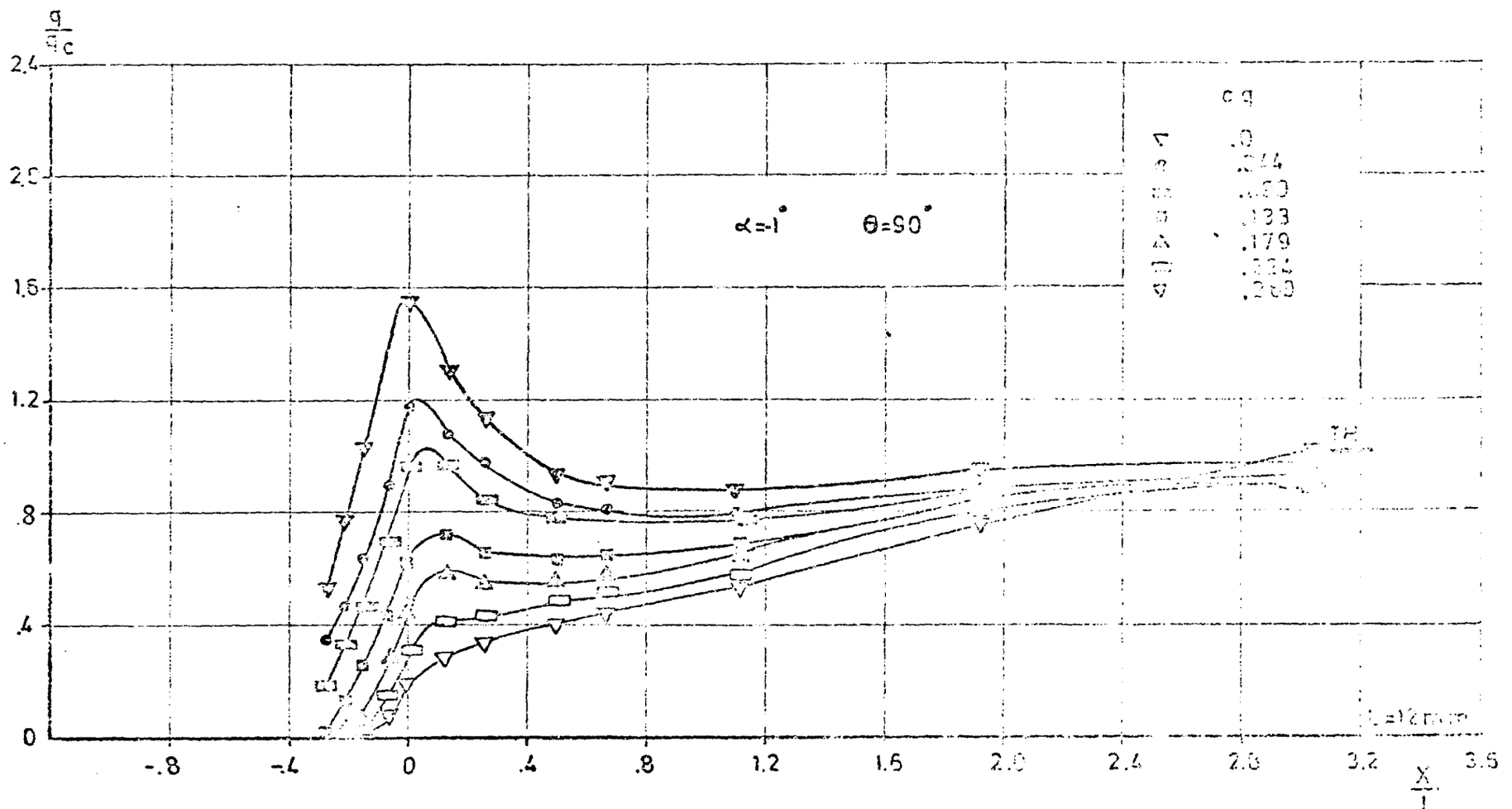

Fig. 3.11 - CONTINUED

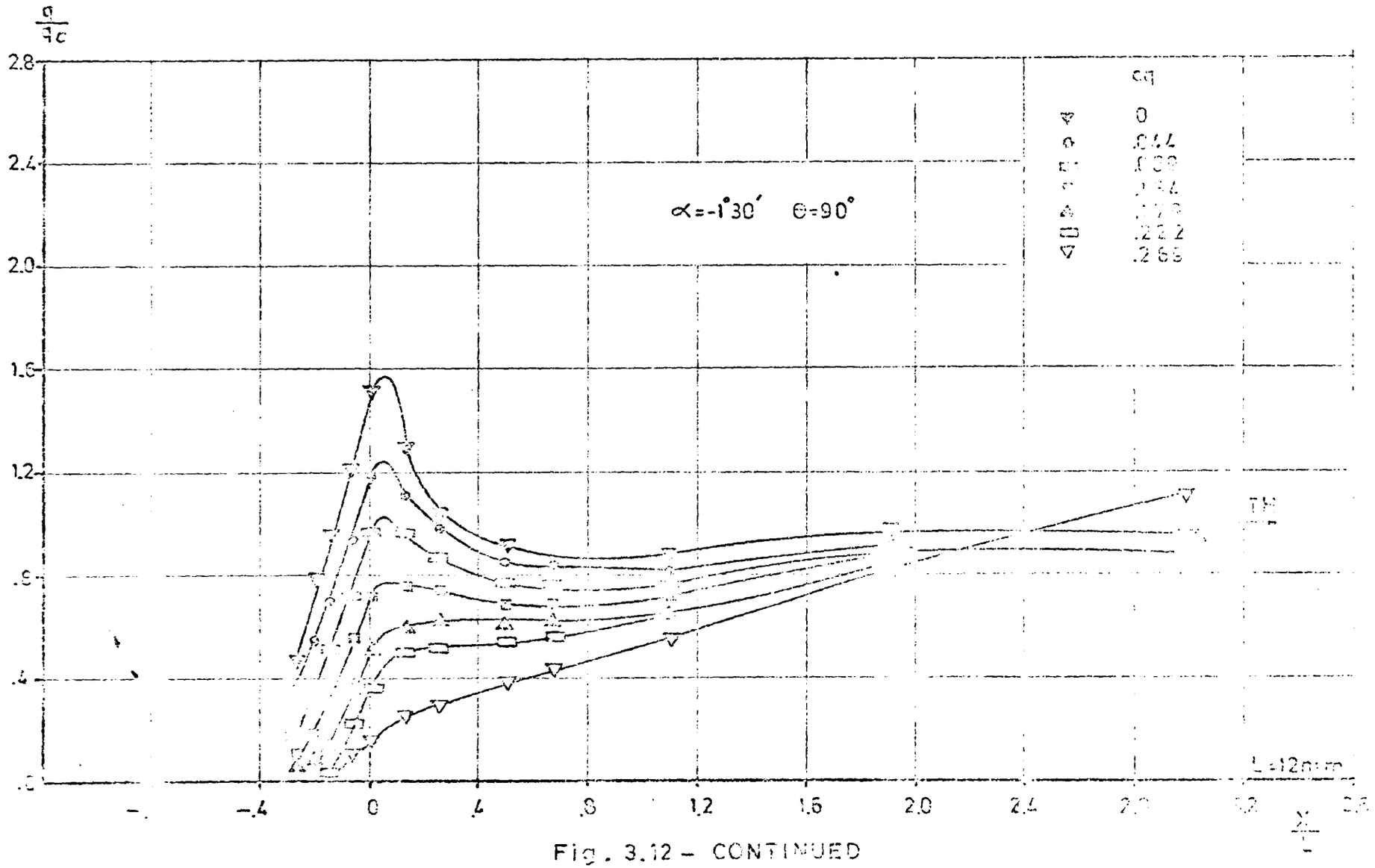

Fig. 3.12 – CONTINUED

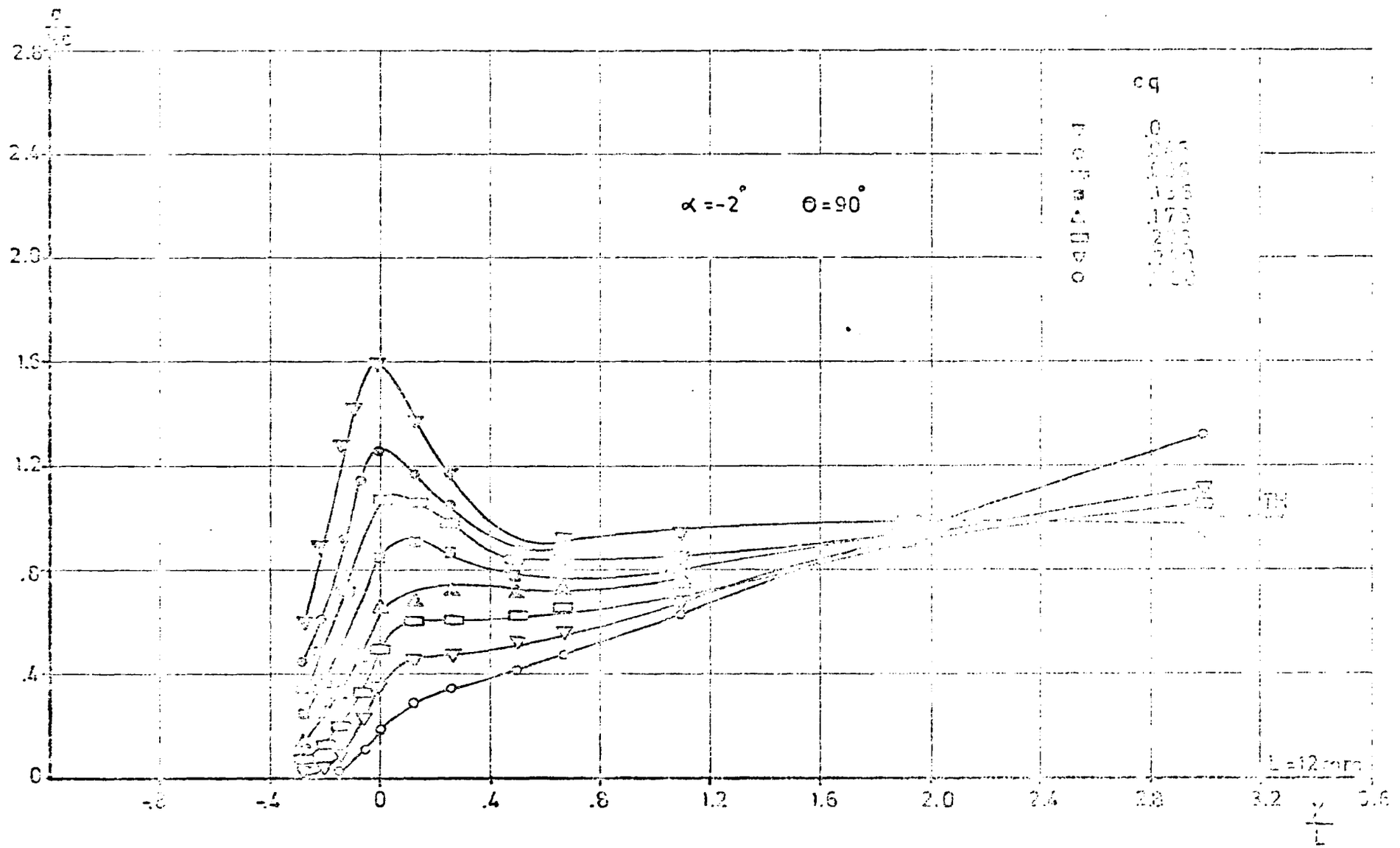

Fig. 3.13 - CONTINUED

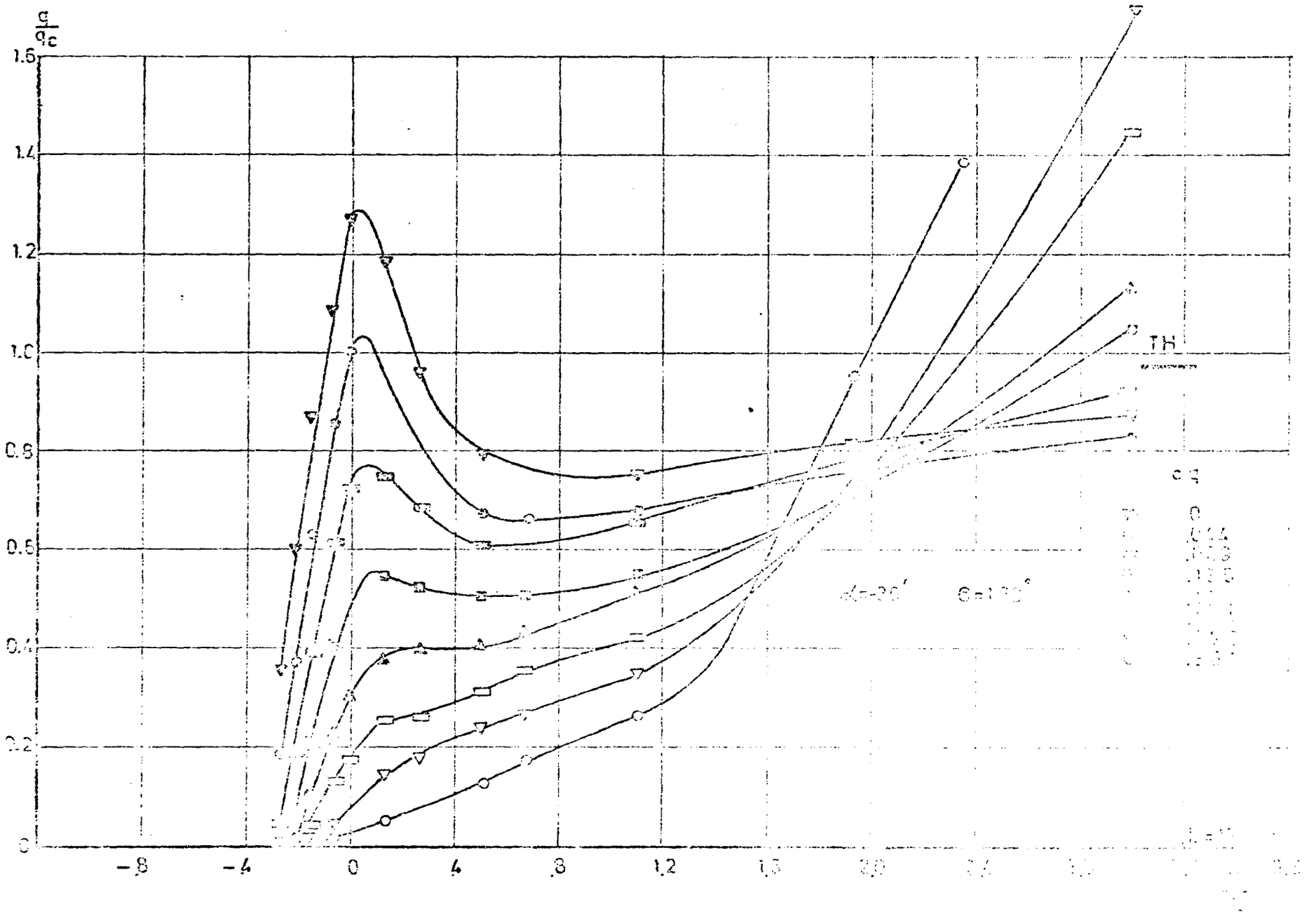

Fig. 3.14 - CONTINUED

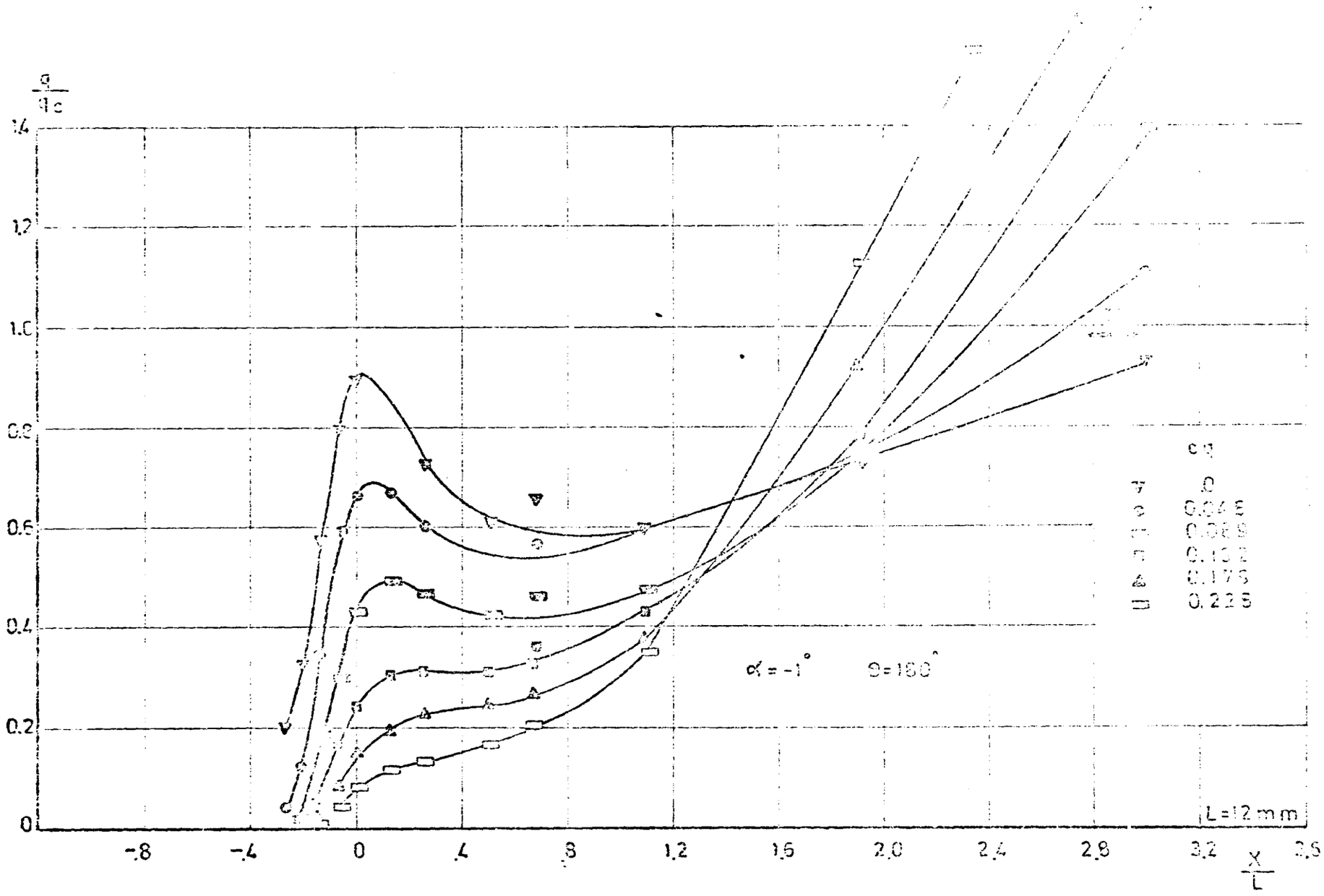

Fig. 3.15 - CONTINUED

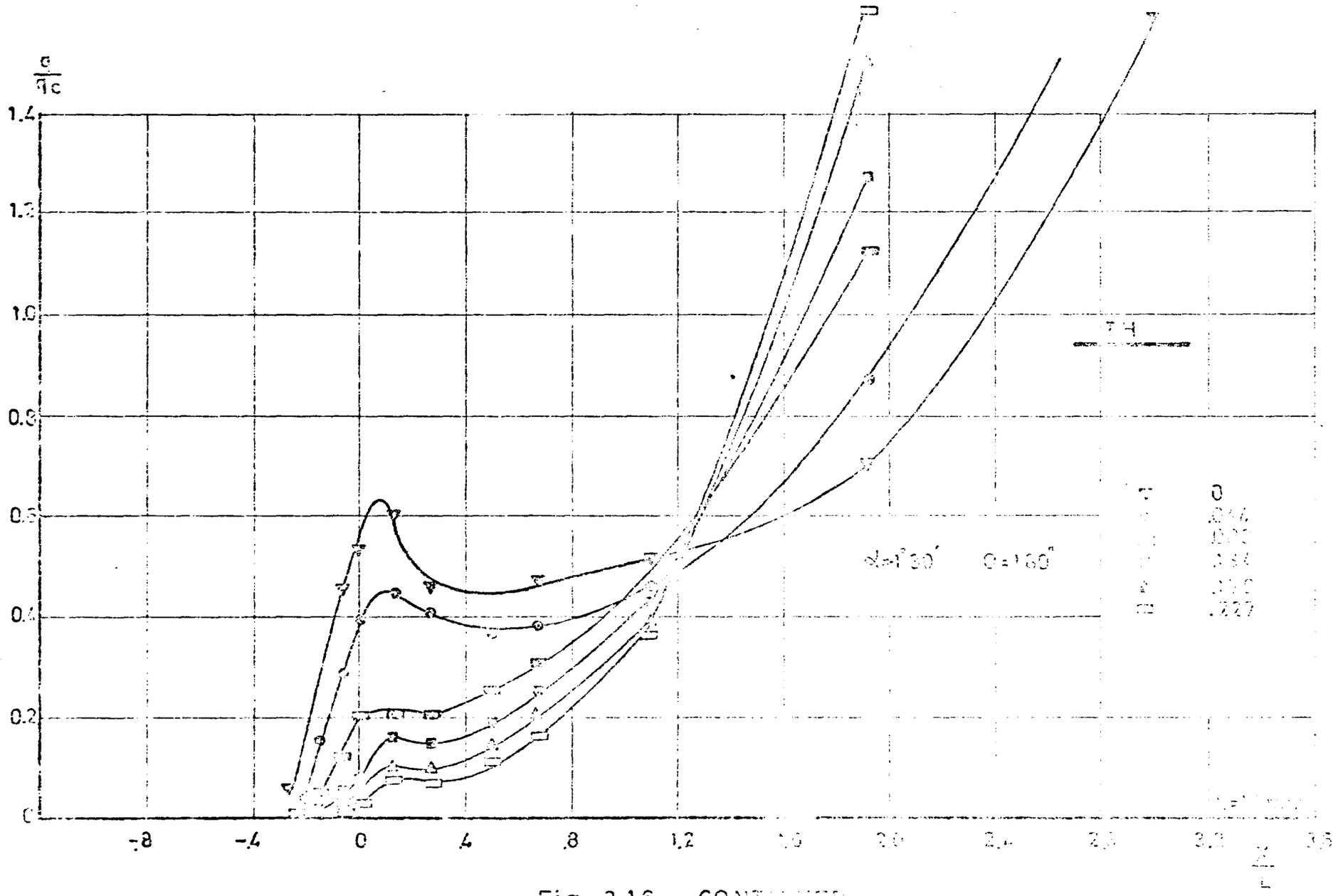

Fig. 3.16 - CONTINUED

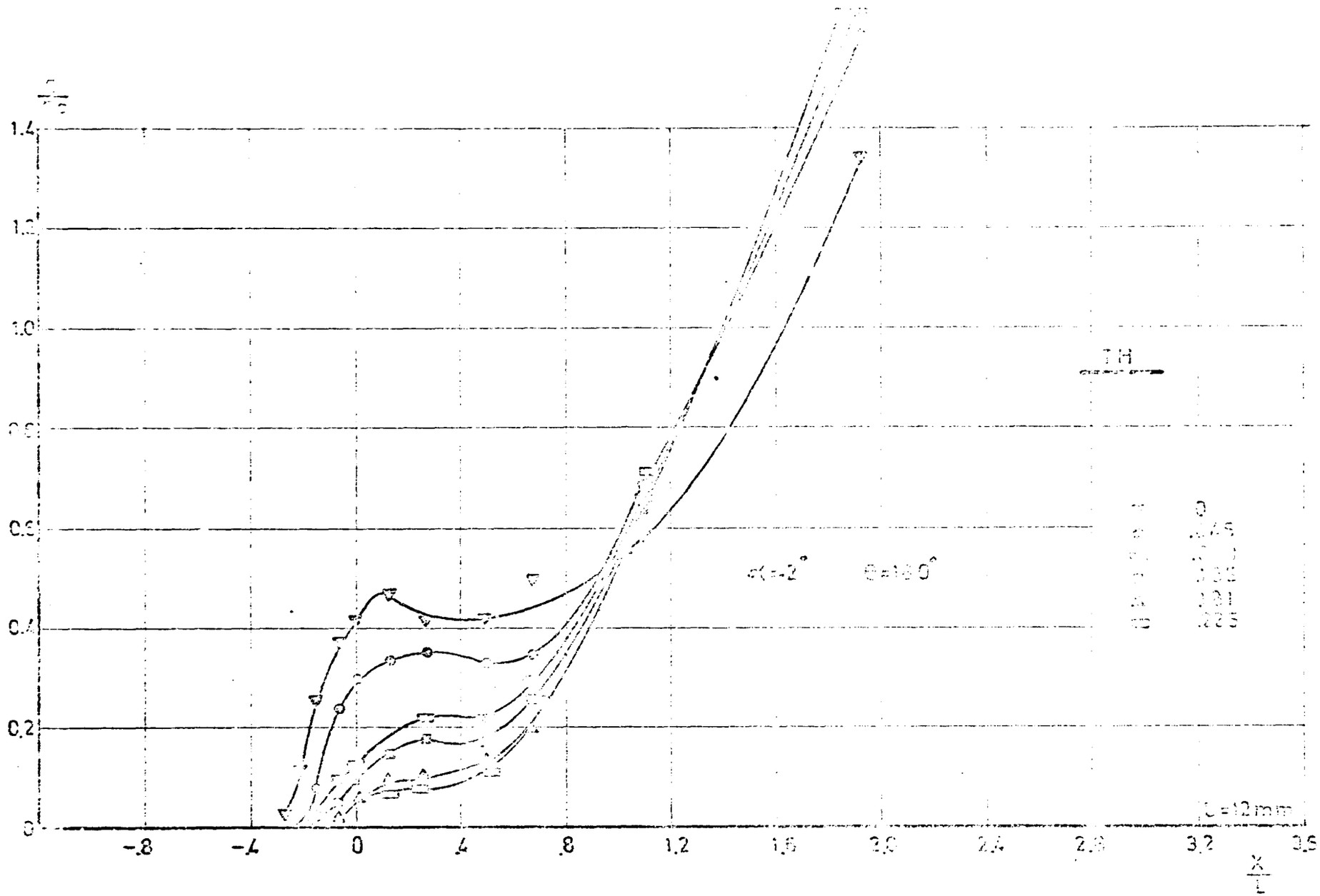

Fig. 3.17 - CONCLUDED

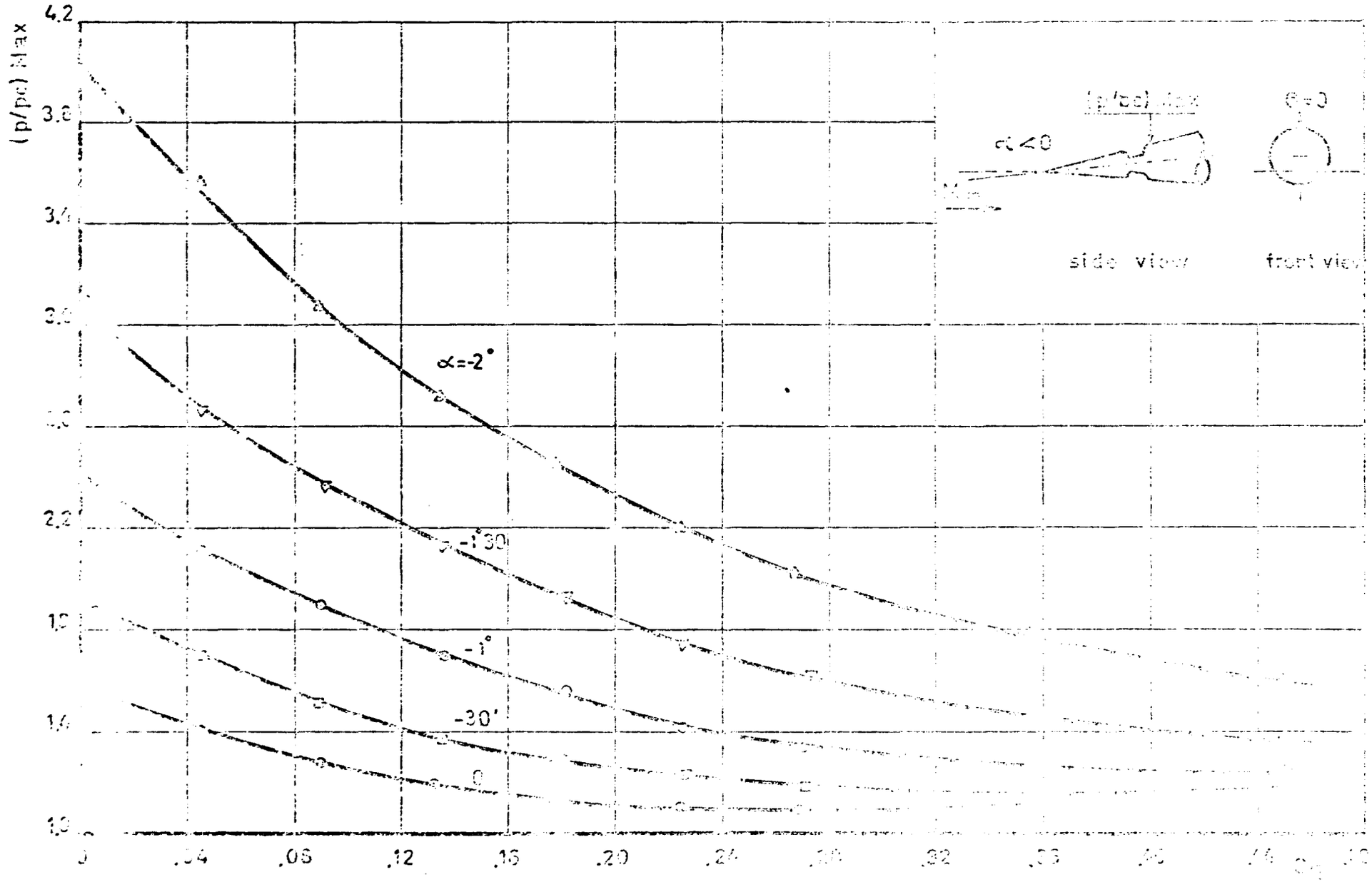

5.41- EFFECT OF AIR INJECTION ON MAXIMUM PRESSURE RATIO

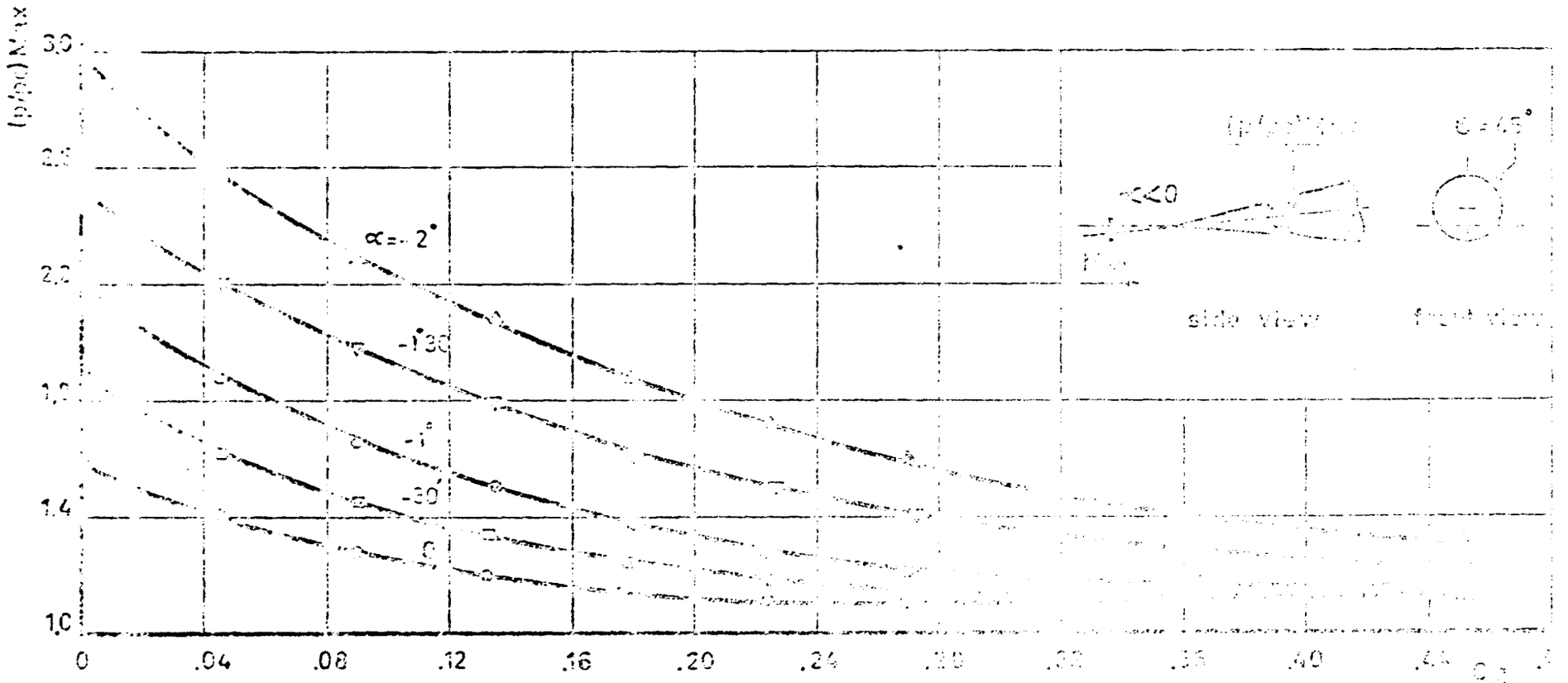

Fig. 4.2 – CONTINUED

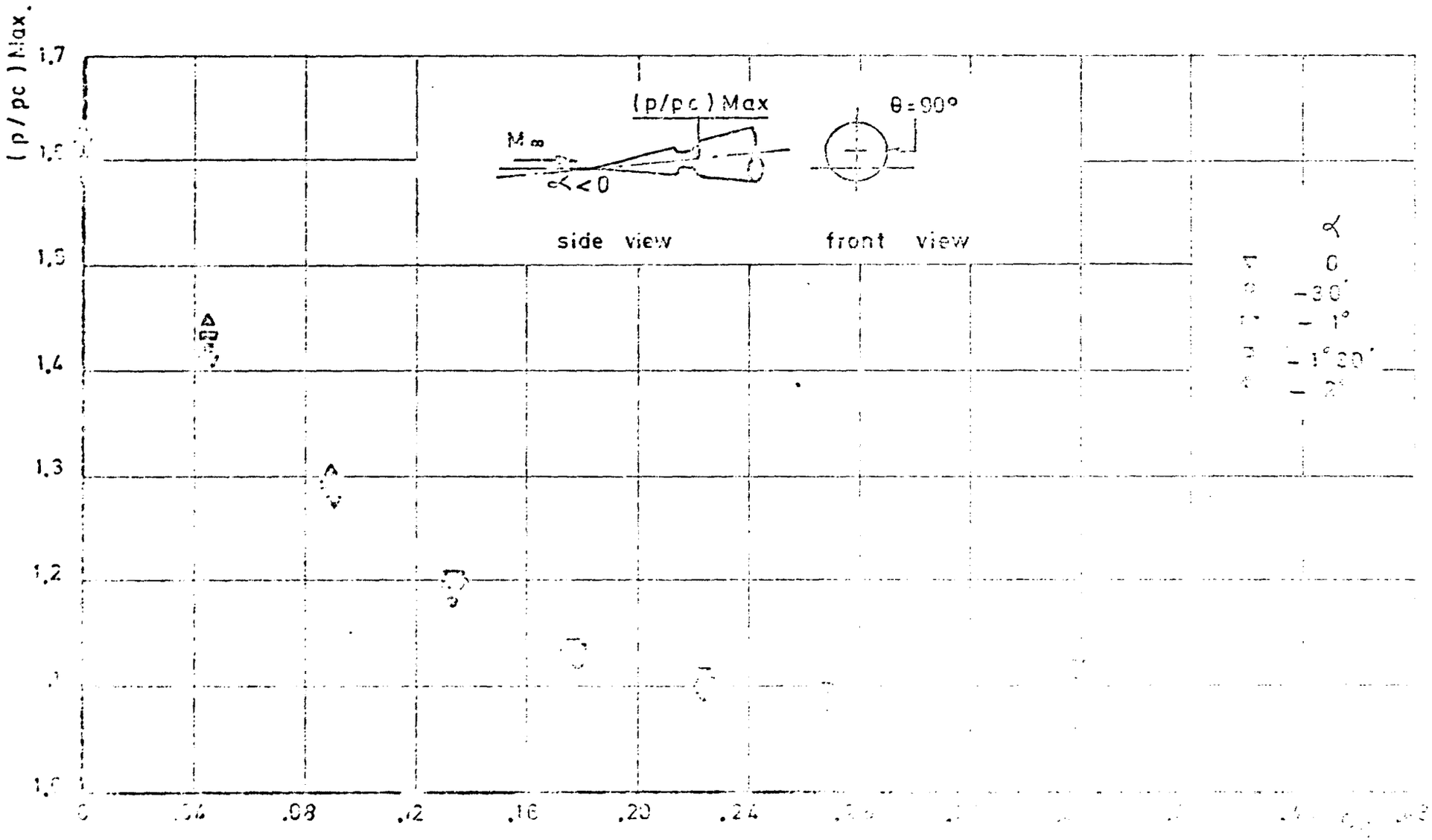

Fig. 4.3 - CONTINUED

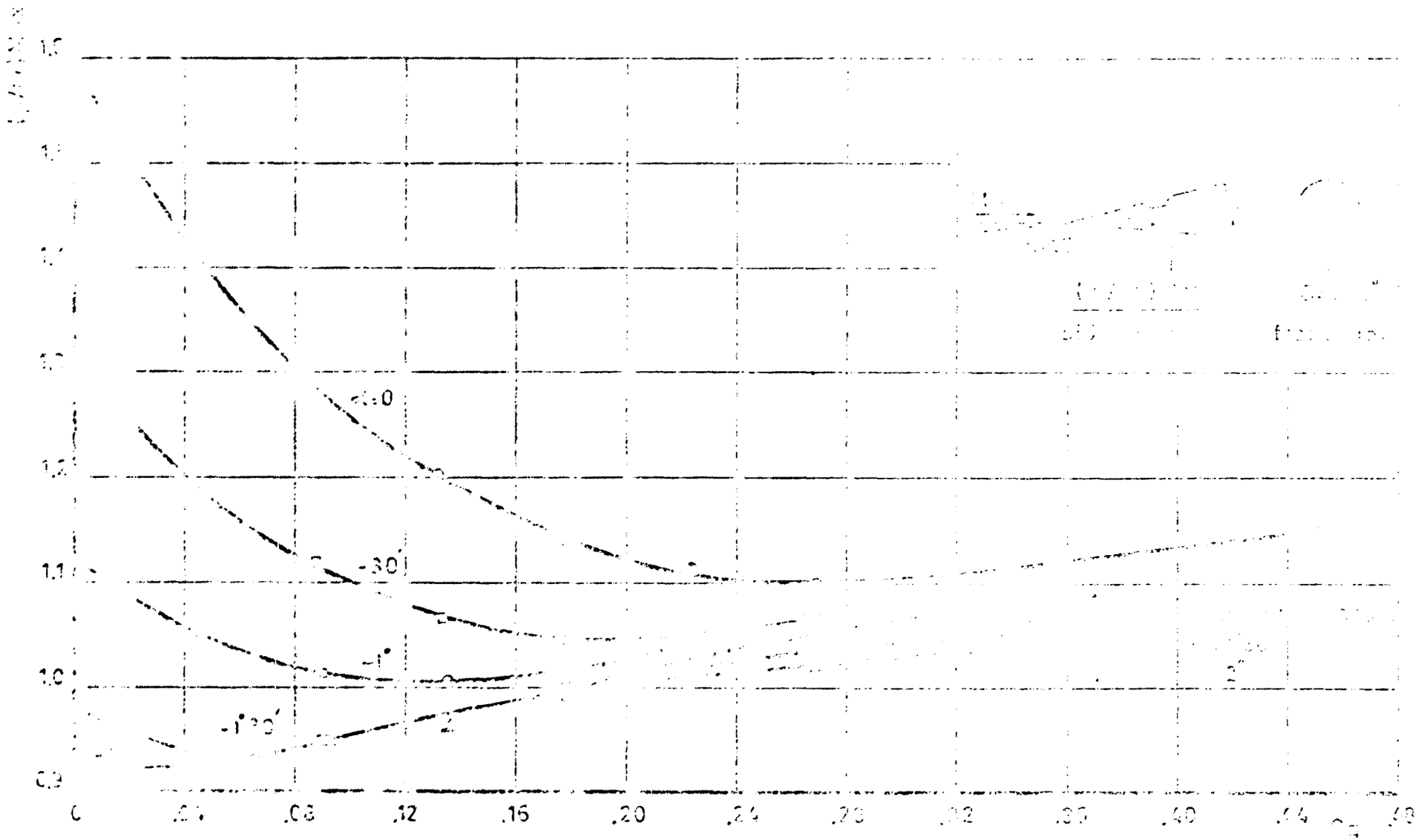

Fig. 4.4 – CONCLUDED

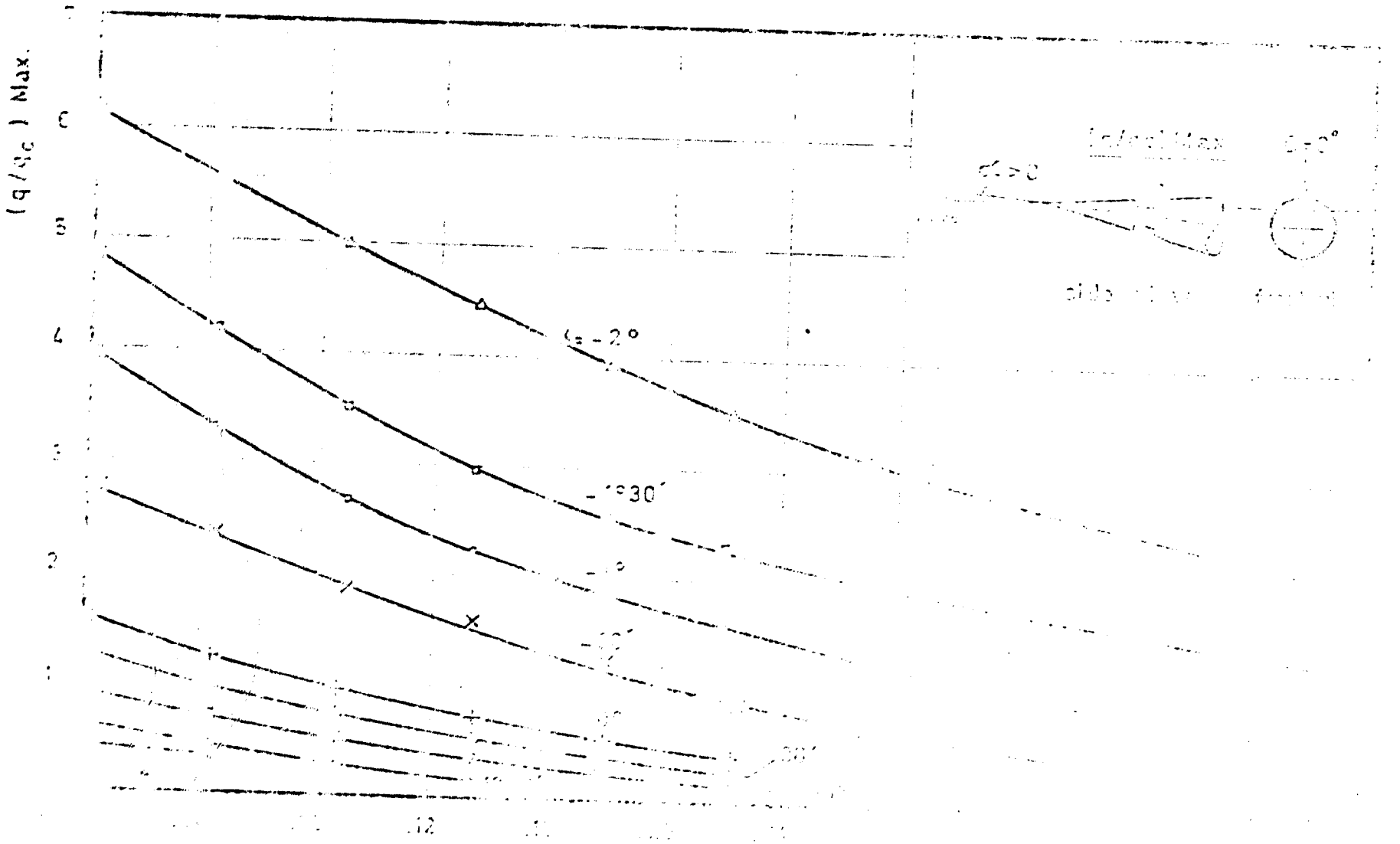

FIG 5.1 EFFECT OF AIR INJECTION ON

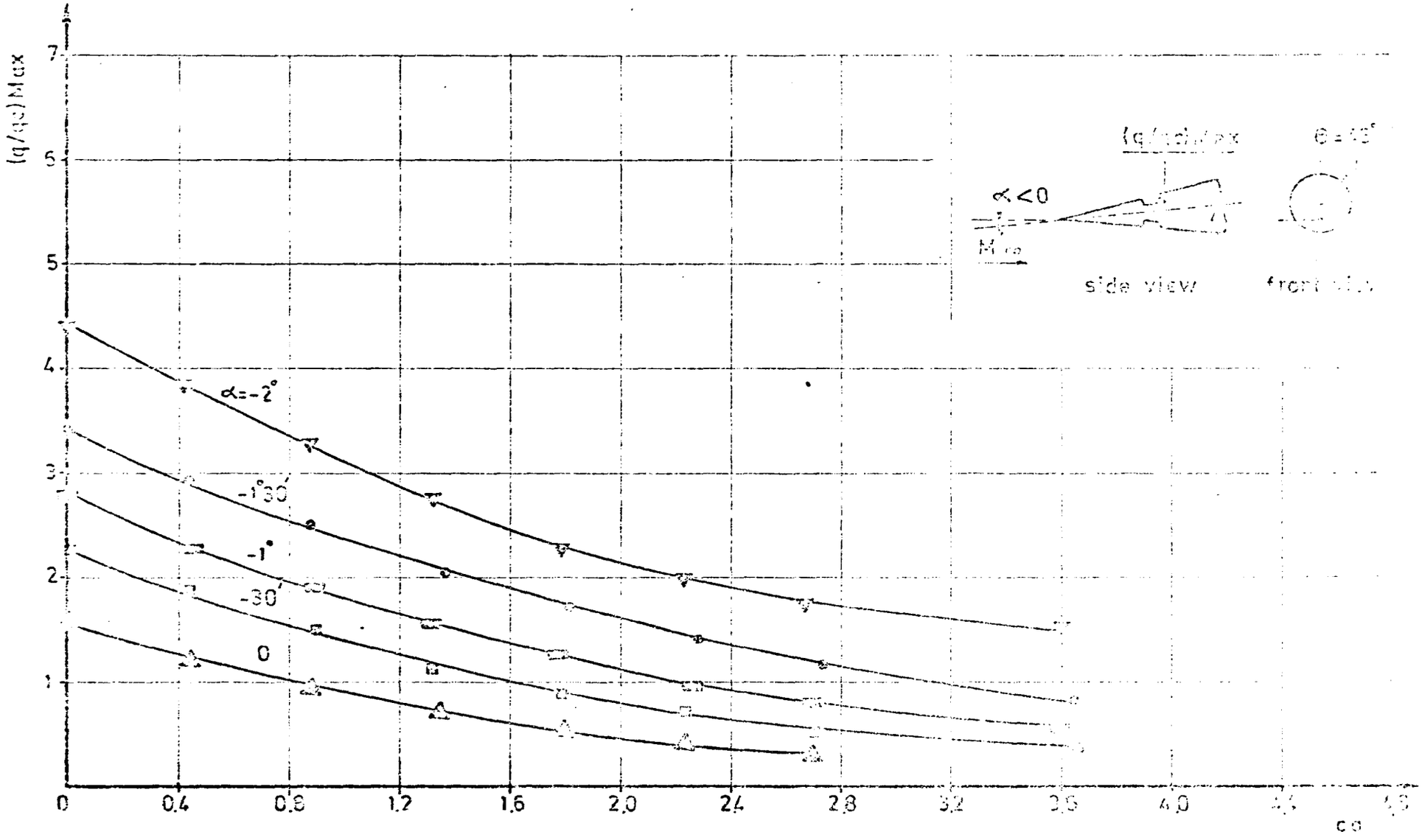

Fig. 5.2 – CONTINUED

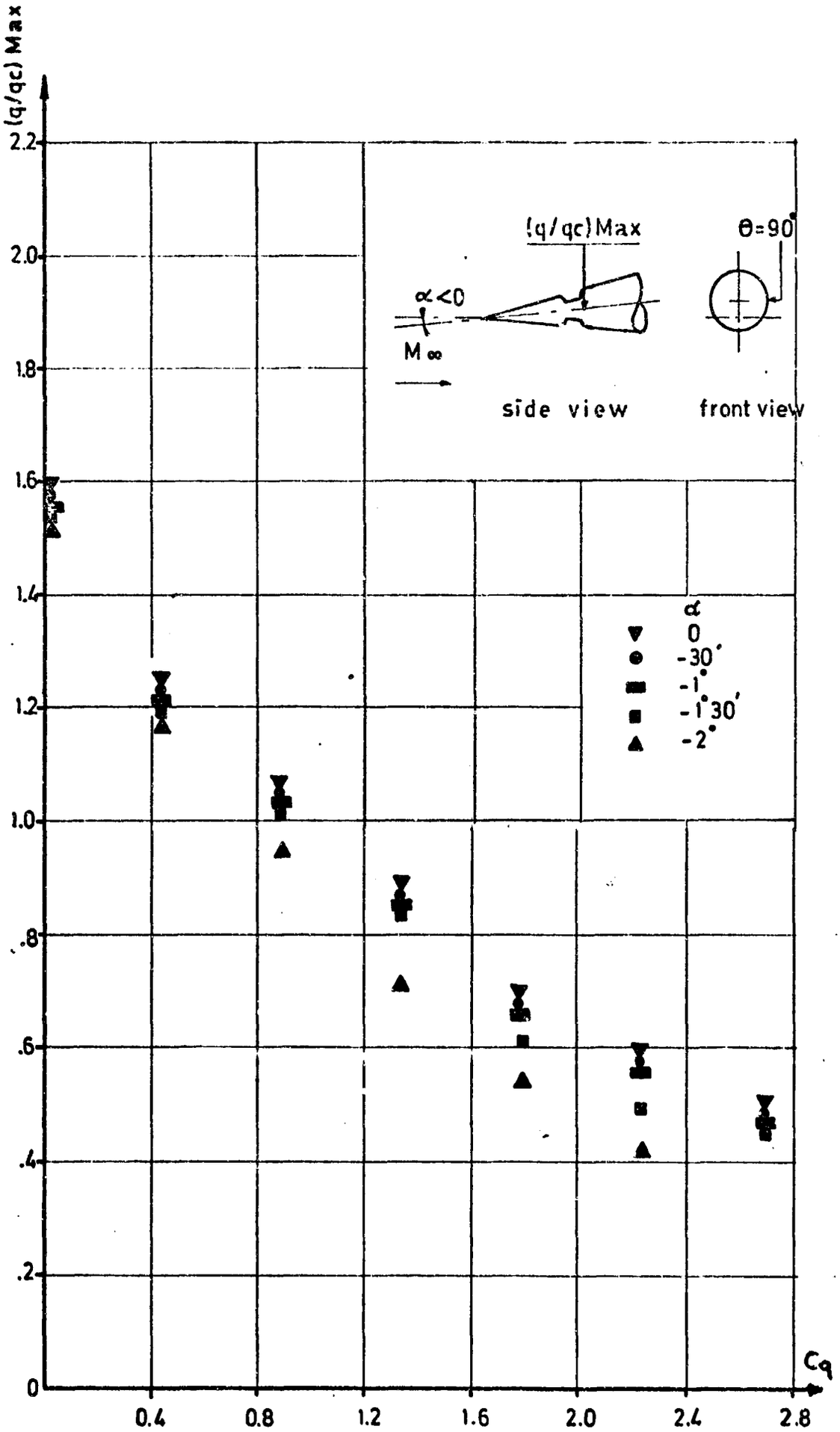

Fig. 5.3 — CONTINUED

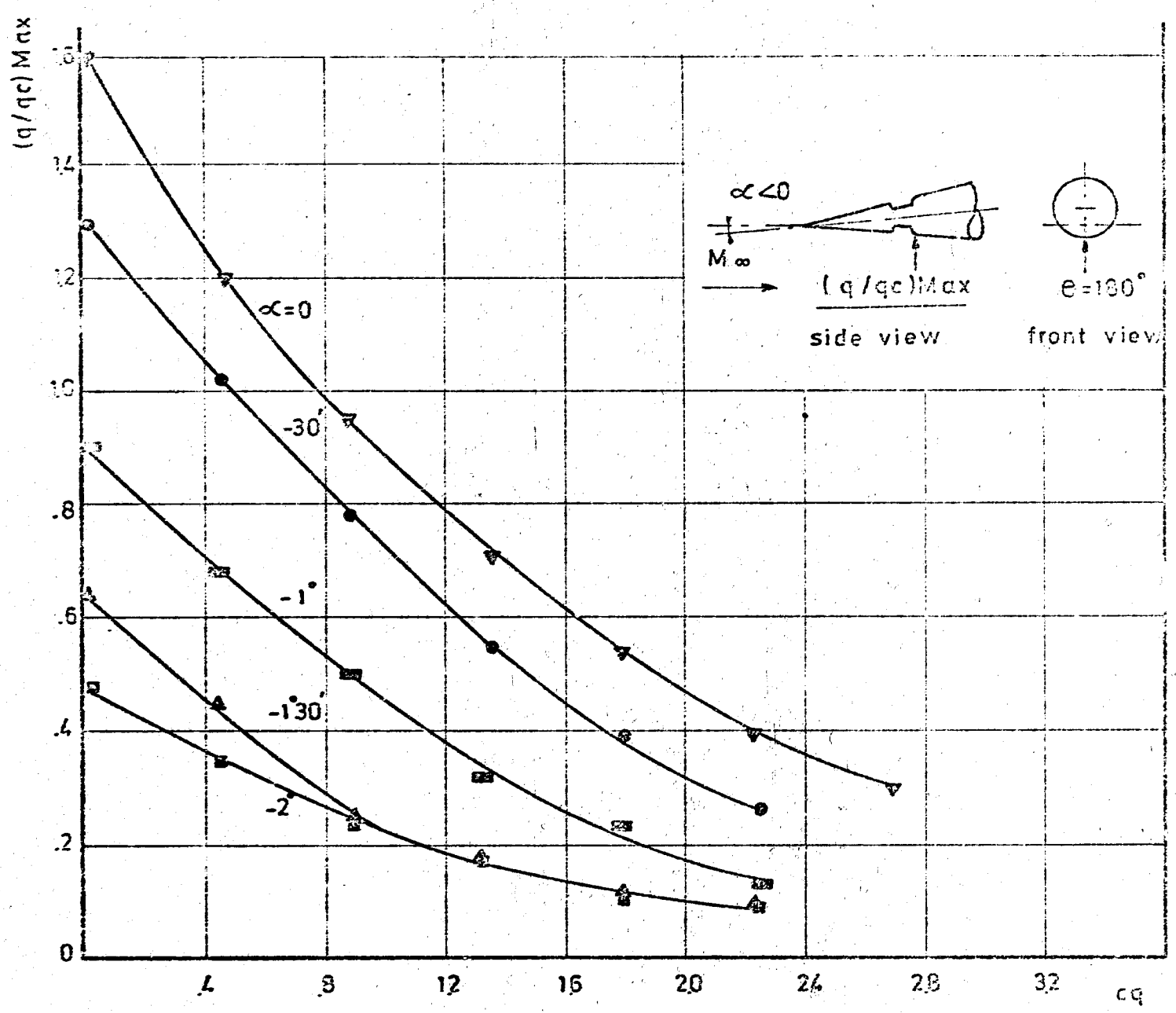

Fig. 5.4 — CONCLUDED